U.PORTO

FEUP FACULDADE DE ENGENHARIA
UNIVERSIDADE DO PORTO

INTEGRATED MASTER IN ENVIRONMENTAL ENGINEERING 2015/2016

OPTIMIZATION OF ENERGY EFFICIENCY IN TERTIARY BUILDINGS

ROGÉRIO RUI DIAS DA ROCHA

Dissertation submitted for the degree of

MASTER ON ENVIRONMENTAL ENGINEERING

President of the jury: Manuel Fernando Pereira
Diretor de curso de Mestrado Integrado em Engenharia do Ambiente da Faculdade de Engenharia da Universidade do Porto

---

Supervisor at the University: Fernando Gomes Martins
Professor Associado do Departamento de Engenharia Química da Faculdade de Engenharia da Universidade do Porto

Supervisor at the hosting institution: Konstantinos Kampouropoulos
Head of Energy Efficiency unit of Sustainability Area of Fundació CTM Centre Tecnològic

Junho, 2016

Abstract

Climate change is widely accepted as one of the most important problems civilization has to deal with. One of its major contributers is the building sector with 32% of the global final energy consumption, 19% of energy-related GHG emissions and 51% of global electricity consumption. The EU set a goal to 2020 of reducing 20% the energy consumption and pointed the building sector as one of the targets and consequently, an area of big either economic, social and environmental interest.

Due to its potencial benefits, energy efficiency optimization is being largely applied in many areas. This dissertation presents an energy optimization method applied on a tertiary building. The methodology includes an adaptive neuro-fuzzy inference system algorithm to calculate a short-term prediction of the building and the sequential quadratic programming algortihm to optimize its energy consumption. The final algorithm is set to optimize the energy efficiency of the building, as well as the operational costs and CO_2 emissions.

The methodology was tested and evaluated in the Fundació CTM Centre Tecnològic using real data.

Agradecimentos

À família, aos amigos, à Fundació CTM Centre Tecnològic e a todos os que contribuiram para a conclusão desta etapa. Obrigado.

Rogério Rocha

"Intelligence is the ability to adapt to change."

Stephen Hawking

Contents

List of Figures

List of Tables

Abbreviations

IPCC	Intergovernmental Panel for Climate Change
GHG	Greenhouse Gases
UNFCC	United Nations Framework Convention on Climate Change
IEA	International Energy Agency
CTM	Centre Tecnològic de Manresa
EER	Energy Efficiency Ratio
AHU	Air Handling Unit
HTW	Hot Tap Water
HVAC	Heating, Ventilation and Air Conditioning
ANFIS	Adaptive Neuro-Fuzzy Inference System
ANN	Artificial Neural Networks
RMSE	Root Mean Square Error
FIS	Fuzzy Inference System
MF	Membership Function
SQP	Sequential Quadratic Programming
CHP	Combined Heat and Power
COP	Coefficient of Performance
UNEP	United Nation Environmental Programme

Chapter 1

Introduction

1.1 Motivation

"We have entered a new era of global cooperation on one of the most complex issues ever to confront humanity. For the first time, every country in the world has pledged to curb emissions, strengthen resilience and join in common cause to take common climate action. This is a resounding success for multilateralism."[1]

UN Secretary General Ban Ki-moon

In December 2015, in Paris, 195 nations reach a long term agreement aiming to limit the global temperature increase to 2 ^{o}C. It is commonly accepted that world's climate is changing and human being is the biggest threat. As a matter of fact, human being is also the only possible solution.
Part of the solution relays on the improvement of energy efficiency that can directly reduce the demand and the associated costs, but has indirect impacts on many other areas. According to [15], energy efficiency has impacts on five main areas: sustainability of the energy system, economic development, social development, environmental sustainability and increasing prosperity. The same document says that the energy use avoided in 2010 was larger than the actual demand of any other energetic supply, including oil, gas, coal and electricity. As a result, energy efficiency became the biggest energy supplier and with no doubt, the cleaner one.
Due to its multiple benefits, optimizing systems have been applied in different areas, including tertiary buildings. This project proposes an optimization process applied to a tertiary building with the main purpose of reducing its energy needs, following the global trend of reversing human impact on the planet.

1.2 Objectives

This thesis was developed and applied in the Centre Tecnològic de Manresa (CTM) with the main purpose of optimizing the energy efficiency of the building. However, the same methodology was

[1] consulted on the 28th of March http://newsroom.unfccc.int/unfccc-newsroom/finale-cop21/

applied to reduce the CO_2 emissions and the total energy costs of the building.
To achieve the purposed goal, the following tasks were fulfilled:

1. Characterization of the Demands
2. Characterization of the Equipment
3. Mathematical Formulation of the System
4. Optimization Process

1.3 Dissertation Structure

The remainder of this dissertation is organised as follows:

- Chapter 2: State of Art
  Describes and analyses the current state of planet's Earth climate; how the energetic and building sector influence it and how energy efficiency can help. Refers also to optimization of energy efficiency systems already applied.
- Chapter 3: Case Study
  Describes the building where the optimization technique was applied.
- Chapter 4: Methodology
  Describes the tools and the procedure that were implemented to achieve the proposed goals.
- Chapter 5: Results and Discussion
  Presents the results of each presented methodology.
- Chapter 6: Conclusions and Future Work
  Presents the thesis contributions and areas for future work and improvement.

Chapter 2

State of the Art

2.1 Background

2.1.1 Global Warming

The Earth's temperature has been relatively constant for the last centuries. This is possible due to a balance with the incoming solar energy and the outgoing radiation. Half of the incoming radiation is absorbed by Earth's surface, 30% is reflected back to space and 20% is absorbed in the atmosphere. In the other hand, the outgoing radiation emitted by the Earth's surface is being highly absorbed by some atmospheric components known as the greenhouse gases (GHG) (such as Carbon Dioxide (CO_2), Methane (CH_4), Ozone (O_3), Water Vapor (H_2O)) and also by clouds which themselves emit this kind of radiation in every direction. This natural phenomenon heats the lower layers of the atmosphere causing the greenhouse effect[6] [17].

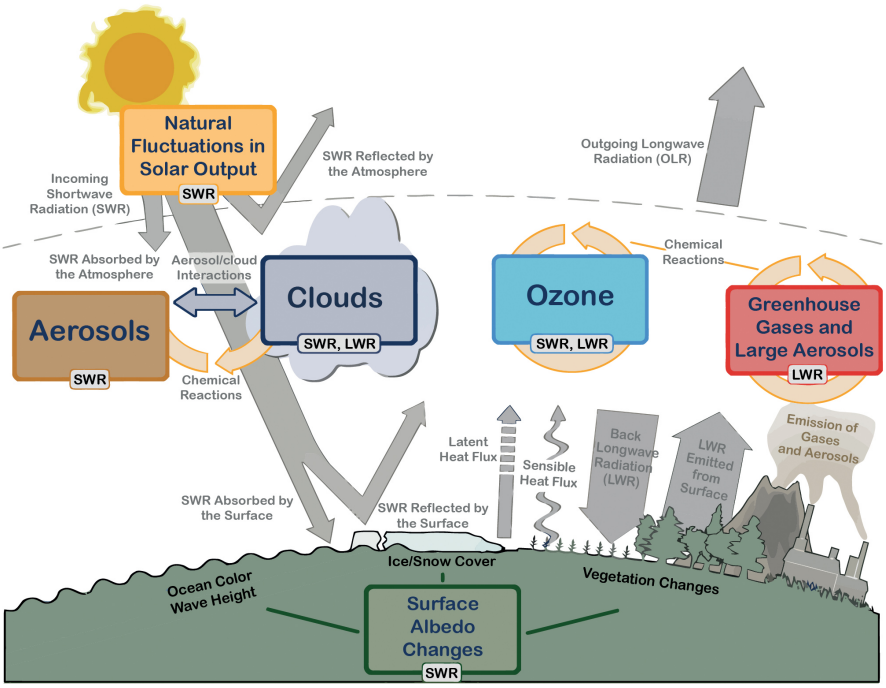

Figure 2.1: Different components of Earth's climate system.
[a]

[a] Cubasch et al, 2013 [6].

There are several indicators of global warming that have impacts on the atmosphere, on the near surface, oceans, land and on ice. Temperature has been lowering on the stratosphere and rising on the troposphere; the concentrations of GHG from anthropogenic emissions has been rising, as well as the tropospheric water vapor; also, there have been changes in ozone concentrations; near the surface, the global average temperature and relative humidity (on land and on sea) has been rising; the temperature has been increasing on much of the world's oceans, such as the global mean sea level; there have been changes in ocean salinity and acidification; more warm days and nights have been registered and there has been reductions in the number of frost days; the snow cover in most regions has been decreasing and changes were observed on large scale precipitation as an increase in the number of heavy precipitation events; the annual average Arctic sea ice extent has been shrinking; widespread glacier has been retreating every year and the ice sheets in Greenland and Antarctica have been rapidly decreasing. Figure 2.2 represents the evolution of some indicators of a global climate change[7] [29] [9].

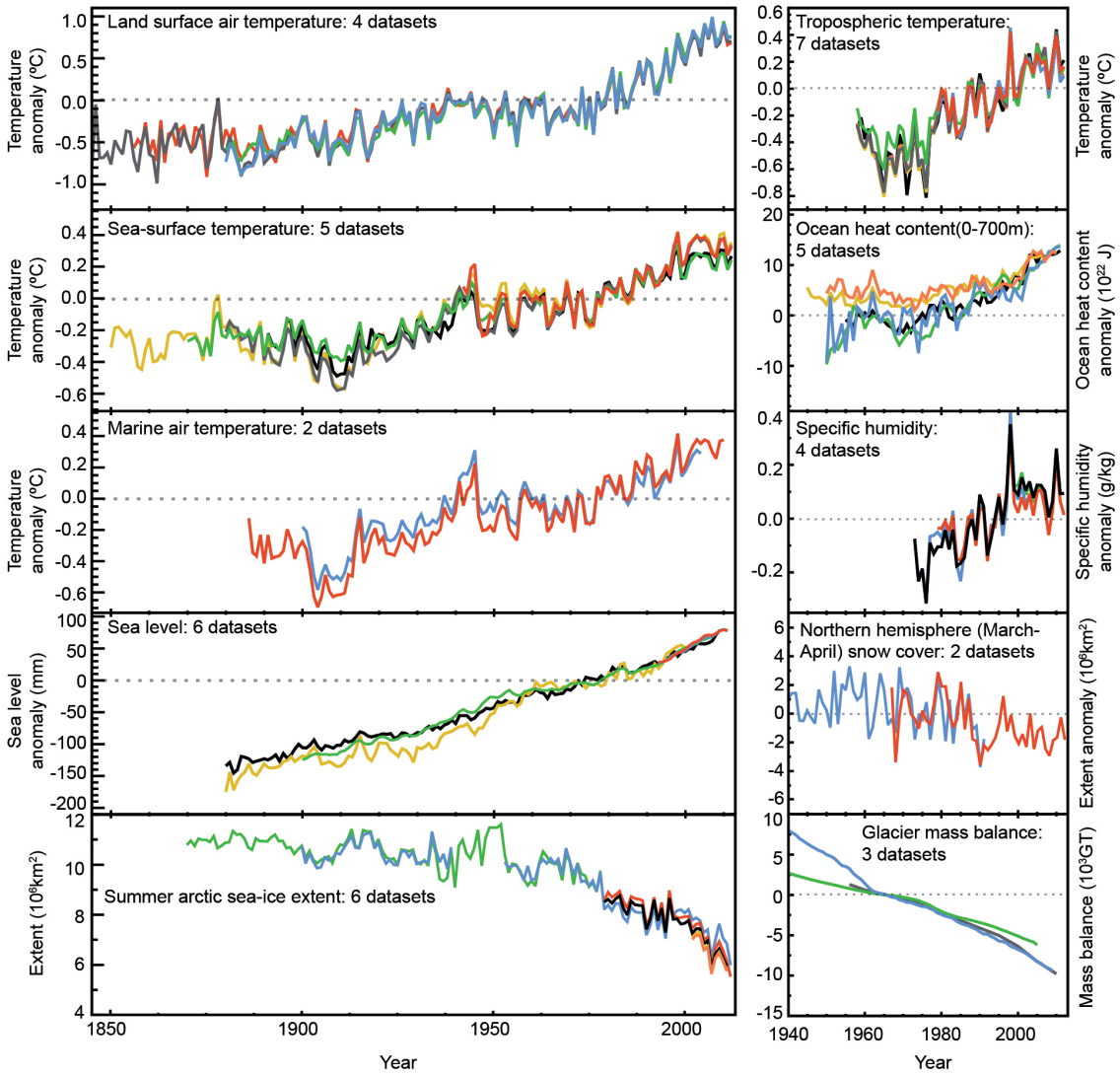

Figure 2.2: Different indicators of climate change and its evolution during time.
[a]

[a] Hartmann et al, 2013 [9].

Figure 2.2 presents variations on some variables that indicates global climate change. Since 1880, the land surface air temperature has increased between 0.650 and 1.06 °C, as well as the sea surface and marine air temperature that also increased. The Arctic sea-ice extent has decreased between 3.50 to 4.10% per decade, which corresponds to 0.45 to 0.51*10^6 km^2 per decade. The same scenario occurs in the Northern Hemisphere snow cover, as satellite records indicate that since 1967 till 2012 there has been a 53.0% loss for the month of June. Additionally, the average sea level has raised between 0.17 to 0.21m, which is a higher rate than what happened in the previous two millenniums. Also, it is graphically represented the increase of the tropospheric temperature, as well as the continuous growth of sea heat content, the increase of specific humidity and the glacier mass balance loss [9].

These indicators are mainly caused by different anthropogenic activities that provoked an exponential increment of the GHG emissions that reached in 2010 the global annual value off 49.50 Gt of carbon dioxide equivalents (CO_2eq), higher than ever before [14]. Figure 2.3 shows the increment of different GHG concentrations in the atmosphere since 1978.

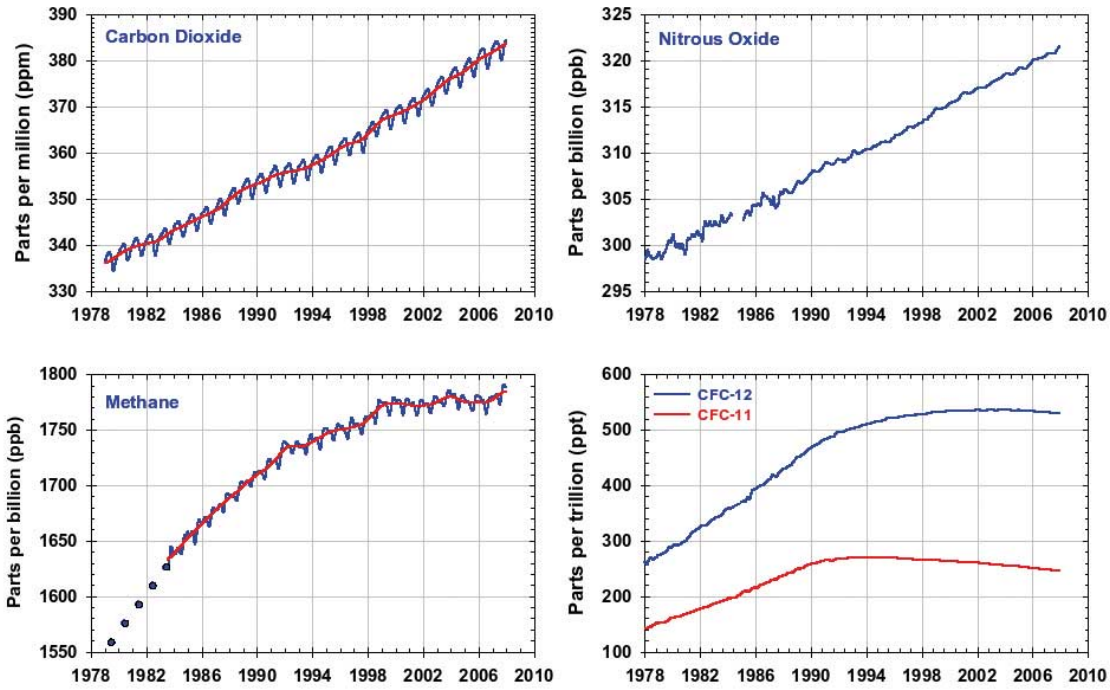

Figure 2.3: Concentration of CO_2, CH_4, N_2O and CFC's on the atmosphere since 1978 till 2010. [a]

[a] http://www.esrl.noaa.gov/gmd/aggi/

In every case presented in Figure 2.3, the increase of GHG's gas concentration is noticeable. In 2011, the concentration of CO_2 increased to $3.91*10^2$ ppm which is 40.0% higher that in 1750. The N_2O and CH_4 concentrations also increased in 2011 to $3.42*10^2$ ppb (20.0% higher than 1750) for the first one and $1.80*10^3$ ppb (150% higher than 1750) for the second [9].
Five major economic sectors are source of these emissions: energy supply, transports, industry, buildings, Agriculture and Forestry and Other Land Use (AFOLU). Figure 2.4 shows the GHG emissions divided by economic sector.

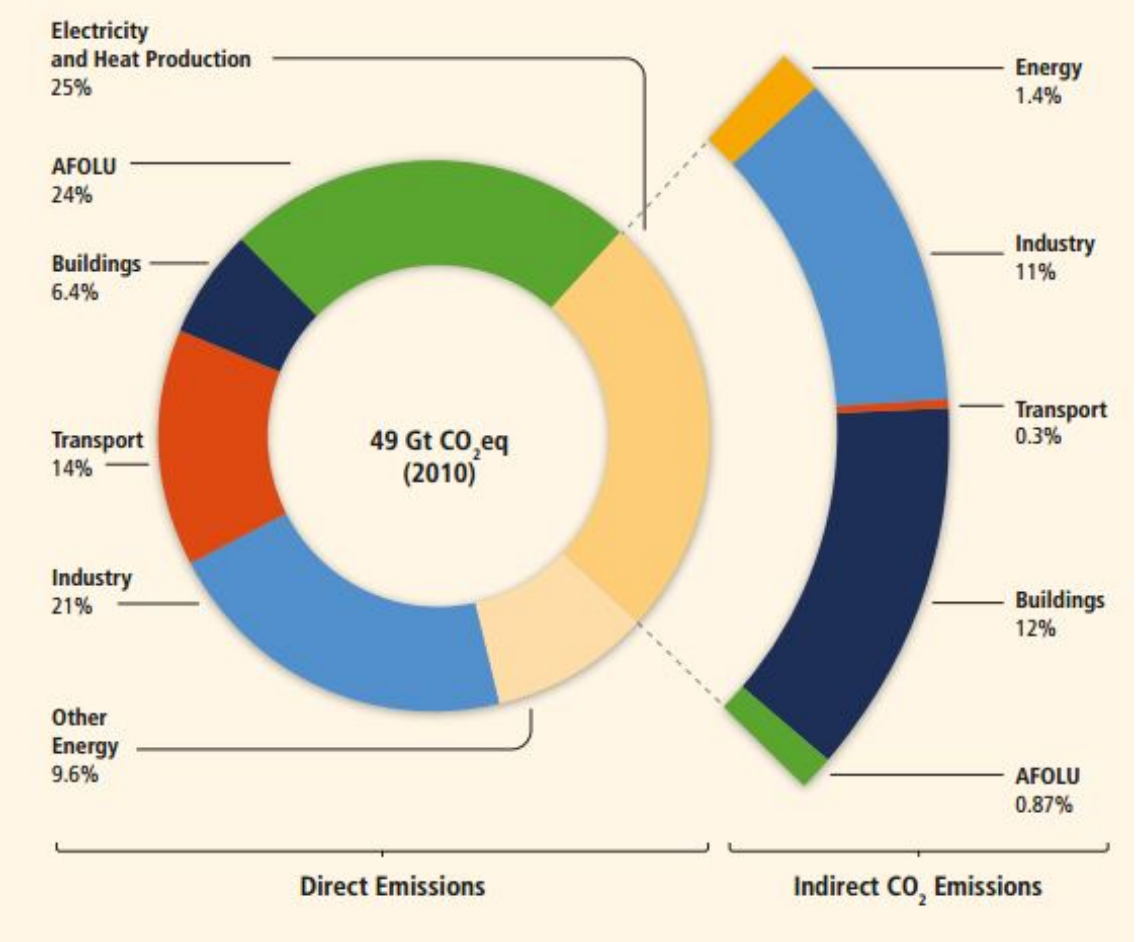

Figure 2.4: GHG emissions by economic sector.
[a]

[a] Edenhofer et al. 2014 [17].

From the 49.5 $GtCO_2eq$ emitted in 2010, 35.0% of GHG emissions were released in the energy sector, 24.0% in AFOLU, 21.0% in industry, 14.0% in transport, and 6.40% in buildings. If it is taken into consideration the indirect emissions from electricity and heat production, the percentage of the industry and buildings sectors grows to 31.0% and 19.0%, respectively. In sum, the energy sector is clearly one of the main responsible sectors for the GHG emissions.

2.1.2 Impact of the Energy Sector

Since the use of steam engines to pump water out of coal mines in the United Kingdom (XVIII century) and later with the development of electric engines (XIX century), the energy sector suffered an enormous revolution till our days and highly boosted the global economy and population growth. The last report of the International Monetary Found (IMF) of January 2016 estimates a global economic growth of 3.10% in 2015 and projects a growth of 3.40% in 2016 and 3.60% in 2017. 70.0% of this increment belongs to emerging markets and developing countries while a slight recovery is being verified in the developed economies [12].

On the other hand, accordingly to the United Nations, world population is set to grow from the current 7.40 billion to 8.60 billion in 2035 and 9.70 billion in 2050. These projections mean more 2.30 billion energy consumers by the year of 2050 and, in the same scenario of the global economic activity, the vast majority of the global population growth will be associated to developing countries, mainly located in Asia and Africa.
These data are important indicators of energy use trends, as by its direct impact through the amount of people that consume energy or how that will happen according with the state of its economy.
As a result, the global total energy supply more than doubled from 1971 to 2012 and, contrarily of what was happening at the beginning of the century, where emissions came almost exclusively from the United States and Europe, today its contribution is less than 30.0%, mainly because of China's contribution (about 30.0%). In the last 27 years, the energy sector emitted as must CO_2 as ever before, as so, it is clear it pays a major contribution to the climate deteoration.
In December 2015, at the 21st Conference of the Parties (COP21), the 196 parties of the United Nations Framework Convention on Climate Change (UNFCCC) reached a long-term agreement in order to keep the global temperature increase below 2 ^{o}C relative to pre-industrial levels. To reach this goal it is necessary to cut between 40.0 to 70.0% of the current total emissions having in consideration the 2010 numbers [27], which will imply a huge transformation in the energy sector, as the energy demand is growing, and is predicted to keep growing [31] (global energy demand is set to grow by 37.0% by 2040 in our central scenario [13]) in order to achieve the established goals.

2.1.3 Building Sector

Throughout history, buildings have shown the level of development of a society, since the first houses till today's complex structures. However, today's challenge in this sector is to minimize the environmental impact of these constructions. Residential and tertiary (services) buildings are one of the most significant contributors of GHG emissions as, in 2010, it was responsible of 32.0% of the global final energy consumption, 19.0% of energy-related [1] GHG emissions and 51.0% of global electricity consumption [2]. Although the majority of GHG emissions comes from developed countries, negative growth rates are observable, contrarily of the positive rate of growth of emissions in developing countries.
In addition, it is important to take into account the life-cycle of buildings and the GHG emissions associated to its different phases. The United Nation Environmental Programme (UNEP) estimates that about 80.0% of GHG emissions associated to buildings, takes place during the operational phase as the remaining 20.0% (varying on the lifetime of the building that can go from a few years to several decades) will be caused by transportation, materials on manufacturing, construction, maintenance and demolition. As referred in Section 2.2, in the next 35 years, the world population is set to have more 2.3 billion people and the vast majority of this growth will take place in developing countries. Consequently, GHG emissions by the building sector may double, or even

[1] If it is taken into consideration the indirect emissions from electricity and heat production, as described in Section 2.1.1.

triple by 2050, if these people won't have access to adequate housing, electricity and improved facilities. The way this is going to happen will influence the future building energy use and the corresponding emissions [16] [11].

2.1.4 Energy Efficiency Relevance

According to the IEA, "Energy efficiency is a way of managing and restraining the growth in energy consumption. Something is more energy efficient if it delivers more services for the same energy input, or the same services for less energy input.". In fact, the IEA believes that the benefits of energy efficiency go beyond the reduction of energy consumption and has influence in areas such as economic activity, employment, energy prices and, consequently, on public budget as the cost would reduce with fuel. Nevertheless, this area is still limited by investment in both private and governmental sectors.
One of the climate and energy policies 20-20-20 [2] is a 20.0% improvement in EU's energy efficiency by the year of 2020 and includes energy efficiency renovations to at least 3.00% of buildings owned and occupied by central governments per year in the EU countries; a reduction of 1.50% in the energy sales of each country per year, among many other measures.
To conclude, the 2015 Energy and Climate Change Report from the International Energy Agency says that the European Union will invest $8 trillion on energy efficiency from 2015 to 2030 where more than one third will be spent on improved efficiency in buildings, emphasizing the relevance of this sector [12] [15].

2.2 Tertiary Buildings and Energy Needs

Despite the heterogeneity of tertiary buildings that includes, among many others, hospitals, schools, the catering industry, houses of worship or the retail sector, the two biggest consumers in this sector are retail and offices. This versatility reflects the diversity of building construction, structures, lifespans and its energy needs [28]. While space heating and cooking are the main end-use in residential sub-sector, in tertiary buildings it is space heating, cooling and lightning that take the biggest shares of final energy consumption, as can be seen in Figure 2.5.

[2] The 2020 package is a set of legislation with the objective of meeting EU climate and energy targets for the year 2020. Besides the improvement on energy efficiency there are included a 20.0% reduction on 1990 levels of EU Greenhouse Gas (GHG) emissions and raising the share of EU energy consumption produced by renewable resources to 20.0%

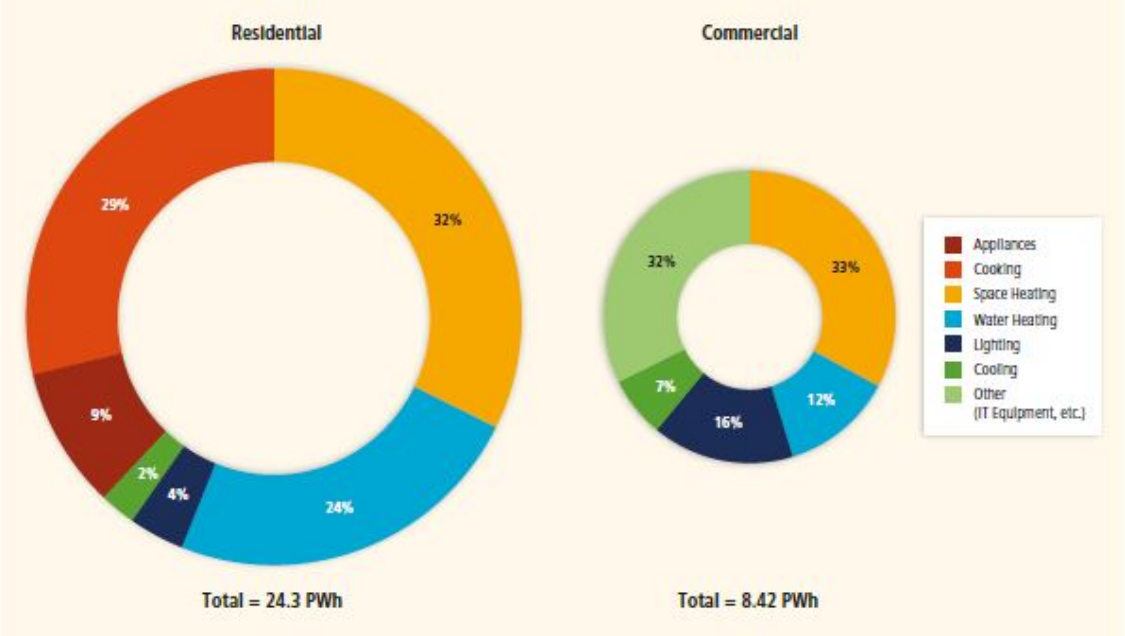

Figure 2.5: Final energy consumption by end-use by the tertiary and residential sub sectors in 2010.

[a]

[a]Lucon et al, 2014 [16].

To maintain a comfortable indoor climate, the vast majority of buildings, including the tertiary ones, use Heating, Ventilation and Air Conditioning (HVAC) systems. There are many possibilities for these systems to work due to the complexity and variety of the equipment involved. Ventilation can occur in a natural way, through the flow of air consequence of open windows, or through mechanical ventilation. Heating can be produced by a boiler, supplied by district heating and/or from Combined Heat and Power (CHP) production. Cooling systems, in a simple way, can be supplied by chillers or throughout small units installed in each room. Finally, Air Conditioning, can combine all the three previous concepts.

In sum, along with lightning, HVAC systems represent the big piece of energy consumption of a building and it is the main indicator of the building's efficiency. In fact, as much energetically efficient a building is, less will be the need for these systems. Figure 2.6 represents the HVAC system applied in the CTM building [21].

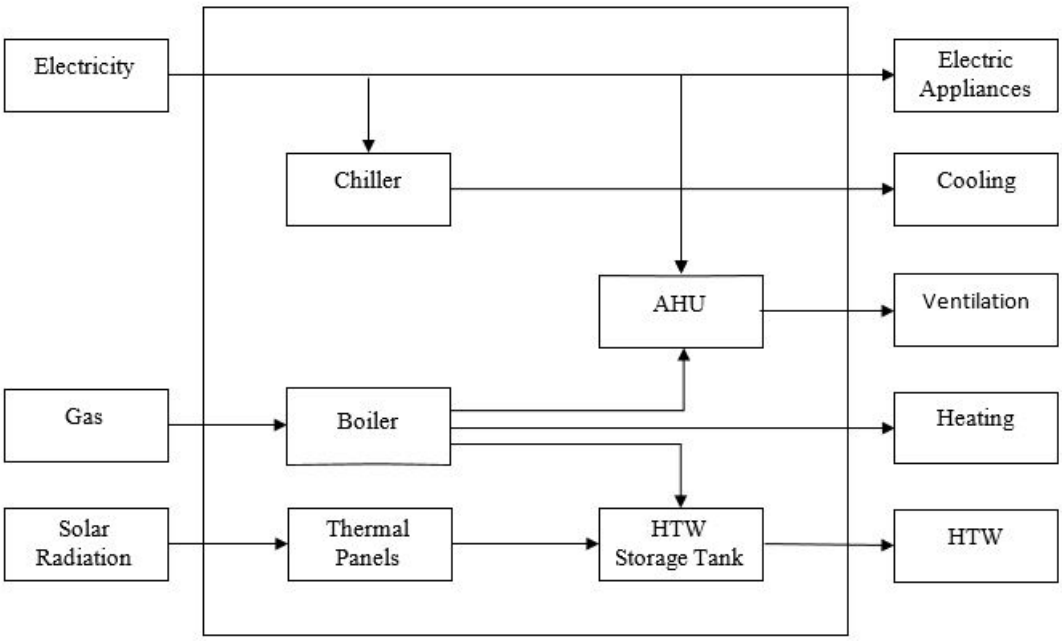

Figure 2.6: HVAC system functioning in the CTM building. In the top of the figure is represented the chiller and above the boiler. Between them, connected by the boiler and the chiller, is represented the AHU.

2.3 Optimization of Energy Efficiency and Areas of Implementation

2.3.1 Optimization of Energy Efficiency

The main objective of this dissertation is to be able to reduce the energy consumption of a tertiary building. This goal follows a global accepted trend of reducing the consumption of energy reinforced, as mentioned in Section 2.1.4, by the long term agreement on keeping the rise of temperature bellow 2 ^{o}C.
Having in mind the continuous developing of the global economy and its relation with the consumption of energy [8], this ambitious achievement can be reached by optimizing the different final consumers of energy.

2.3.2 Areas of Implementation

The areas of higher consumption of energy in the world are, in order of relevance, industrial users (such as textile, food, drink and tobacco or mining), personal and commercial transportation and residential and tertiary buildings [26]. As so, due to its potential benefits on reducing costs, emissions and consumptions, several research on these areas have been conducted. In 2014, Mahoor et al. [22], it is presented a smart street lighting system through wireless control to reduce the energy consumption as well as the maintenance costs, GHG emissions and increase the lamp life;

in 2006, Acampora et al [1], applied an optimization procedure based on an on-board monitoring system that measures the electro-mechanical data of the train and previously send it to a control station through a network connection with the objective of reducing the energy consumption; a different model was applied in Bozic in 2007 [4], aiming to understand and optimize the specific energy needs on an island in Croatia (space heating, hot water, cooking, air conditioning and specific electric consumption - for lightning, washing and drying, freezers etc). Furthermore, in Gao et al in 2010 [35], it was predicted the comfort levels based on HVAC systems performance and climatic conditions; optimization of energy efficiency was also applied on areas as robotics like by Vergnano et al in 2012 [30], or on industrial plants by Kampouropoulos et al in 2014 [20], where was combined an adaptive neuro-fuzzy inference system and a sequential quadratic programming algorithm to optimize the operational and maintenance costs and the CO_2 emissions.
To conclude, the implementation of optimization systems with the aim of reducing the energy consumption and, consequently, the costs and emissions, is increasing in the last years due to its potential, versatility and coverage of areas of implementation.

2.3.3 Optimization of Energy Efficiency in Tertiary Buildings

In Section 2.1.4 is referred the "20-20-20" EU policy where it is included a 20.0% reduction on energy consumption by improving energy efficiency. One of the areas of implementation of this policy is the Building Sector, one of the economic sectors with highest impact on the world's climate as described on Section 2.3. To emphasize this fact, the European Commission defined the objective of only net-zero-energy buildings shall be constructed in the Euro zone after 2050.
The biggest shares of energy consumption in tertiary buildings are related to heating, cooling and lightning so, as a result, optimization is mainly applied on these areas. There are different approaches being tested to reach the goal of reducing energy consumption. Sahyoun et al in 2012 [25], used a distributed parameter model to control the temperature of rooms; Brenna et al in 2012 [5], tested a new concept of smart grid with the aim of obtaining a optimized and integrated management of services; Weiss et al in 2015[32], Bhandari and Ridge in 2012[34], Meckler et al in 2014[23], Boeke and Ott in 2014[3] and Wunder in 2014[33] proposed different ways to distribute electricity in buildings and grids and claim to demonstrate at least 5% on energy savings and 7% on increasing the efficiency of solar power systems.

Chapter 3

Case Study

3.1 Fundació CTM Centre Tecnològic

This thesis case study is the Fundació CTM Centre Tecnològic, a three store building (considering the basement) which occupies an area of 4542 m^2.

Figure 3.1: CTM building.

The equipment which operates in the building that was relevant to the dissertation is presented as follows:

- Thermal Solar Panel

  In total there are 3 vacuum tube thermal solar panels with a total area of 8.60 m^2.

- Chiller

  The building possesses 1 chiller with a thermal power of 789 kW and an electrical power of 271 kW. Figure 3.2 shows us the chiller and the thermal solar panels disposed on the roof of the building. The chiller in the ground floor is presented on Figure 3.4.

Figure 3.2: Thermal solar panels (above) and chiller (bellow) of CTM building.

Figure 3.3: Chiller in the ground floor.

- Air Handling Unit (AHU)

Table 3.1 presents the technical characteristics of the two AHU that includes the cold and hot water circuit and the return and blower fan.

Table 3.1: Characteristics of the Air Handling Units of CTM building.

	Cold Water Circuit		**Hot Water Circuit**		**Return Fan**		**Blower Fan**	
	Total Power (kW)	Temperature Variation (^{o}C)	Heat Power (kW)	Temperature Variation (^{o}C)	Electrical Power (kW)	Flow (m3/h)	Electrical Power (kW)	Flow (m3/h)
AHU1	61	[7-12]	64	[55-65]	3	8400	4	8400
AHU2	47	[7-12]	50	[55-65]	2.2	6500	3	6500

Every hour between 10 to 25% of the air is renewed every hour, which means that between 4 to 10 hours the air is totally renewed in the building.

- Boiler

There are 3 boilers (see Figure 3.5) operating in the ground floor of the building with a total power of 295 kW. Two of them have a nominal capacity of 90 kW and the other 115 kW. They both operate with a 85% boiler efficiency.

Figure 3.4: Boilers in the ground floor.

CTM has an intelligent energy supervisor system that provides real time data of consumption and demand of the building, as well as meteorological data monitored by a meteorological station, installed in the roof of the building. A scheme of this system is presented on Figure 3.6.

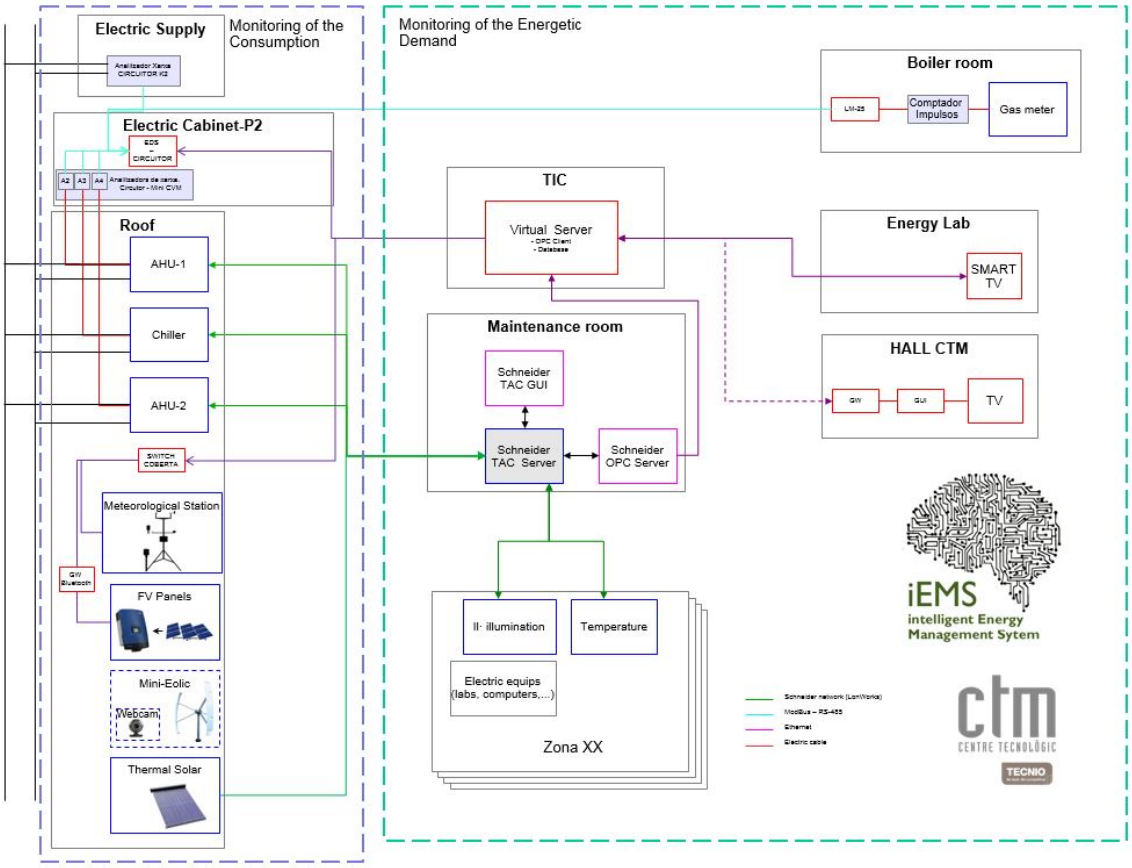

Figure 3.5: CTM energy supervisor system.

The meteorological station in the lower-left corner is connected to the maintenance room, as well as the the chiller and AHU's, that are connected to the Visual Server in the middle, making the information easily available. Furthermore, the data information of the Boiler, in the upper-right corner, and the electrical supply, in the upper-left corner, connects with the electric cabinet that also sends its information to the Visual Server.
Grafana, a web service platform, displays the information stored in a database. CTM uses influxDB, a type of database oriented to temporal data series where all entries are meant to be stored sequentially in time. To contain information of the 4 seasons, the information is stored maintaining a maximum historical period of 1 year.

3.2 Energy Hub

In this project, the energy hub concept is defined as a way to represent the relations between the different energy flows and the HVAC equipment in the building, so as to understand the several transformations and transportations that the different energy flows undergo from the input until its final deliver.

Figure 3.7 shows the scheme of the energy hub operating in the CTM building with the inputs, outputs, equipment and its relations that are relevant for this dissertation.

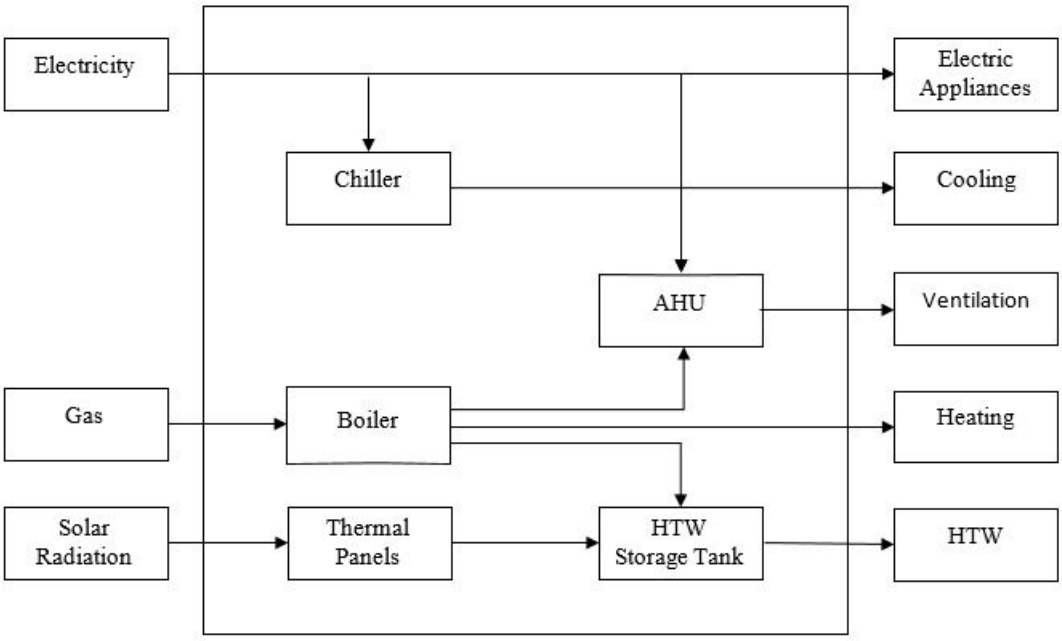

Figure 3.6: Energy hub scheme of the CTM building with inputs in the left and outputs in the right.

As can be seen in the Figure 3.6, on the left, there are three suppliers of primary energy [1] to the equipment of the CTM building: electricity, gas and solar radiation. The building energy demands (heating, cooling, ventilation, hot tab water and electric appliances [2]) are represented in the right and the different equipment and its relations are schematized in the center of the figure.

[1] Primary energy concept refers to energy sources found in nature that weren't subjected to any transformation processes. In this case it refers to the energy that is taken outside the system.

[2] The electric appliances are every equipment turned into electric current such as computers, lab equipment, canteen machines, TV's, lightning etc.

Chapter 4

Methodology

4.1 Overview

As described in Section 3.2, the energetic infrastructure of the building is characterized by three different parts: the energy supplies, the equipment responsible for the energy production and its conversion and the demands. Due to its installations and processes (i.e. laboratories, HVAC conditions, etc), the building has specific energy requirements that cannot be reduced, so the energy savings is applied on the primary energy sources (energy supplies). Thus, this dissertation is focused on the energy flow optimization into the system (determine how much of each type of energy has to flow through the different available carriers, in order to consume less energy). The control of the flow is made by controlling the operation of the conversion and production equipment.
The following sections describe the four steps that took part of the project. First, it is explained the characterization of the demands of the building through the application of a predicting algorithm along with its structure, as well as the data treatment that precedes the modelling; next, the procedure to characterize the efficiency of the equipment is described containing the different possible approaches; then, the equations and restrictions of the system are presented and finally, the optimization process is presented in detail.

4.2 Characterization of the Demands

4.2.1 Pre-proceeding of data

As in every HVAC system, the demands of the building (represented in Figure 3.6) are cooling, heating and ventilation, but for this project are also considered electric appliances and HTW. These data were acquired by using different energy meters and sensors into influxDB, making it available for consultation. Additionally, two meteorological variables were considered to predict the behaviour of the building in terms of consumption and production. The considered variables were the solar radiation and the temperature outside the building.

- Synchronization process

As mentioned in Section 3.1, the intelligent energy supervisor of the building consists of different sensors and acquisition systems (e.g. electric measurement, heating demands, weather conditions, setpoints, etc) that work individually. As a consequence, the information is registered in different timestamps that obligates a synchronization process between the considered variables for the project so that every entry is synchronized in time with each other. This process consists on the analysis of the time vector of each variable and convert it into 96 points per day, which corresponds to a 15 minute frequency between each entry. The conversion of the value vector of each variable into 96 points per day requires a sum or mean calcutation depending on the variable (for the meteorological data was applied the mean and for the demands variables the sum).
Table 4.1 exemplifies a synchronization process applied to the values of the consumption of the total cooling demand of the building between 17:31 and 18:00 of the 2nd of November of 2015.

Table 4.1: Total cooling demand values before and after the synchronization process.

Time	Consumption (kW)	Time	Consumption (kW)
17:31	218.65	17:45	909.67
17:32	178.43		
17:33	116.55		
⋮	⋮		
17:45	30.94		
17:46	9.28	18:00	907.62
17:47	15.47		
17:48	21.66		
⋮	⋮		
18:00	133.05		

As can be seen in the 2 columns in the left, the total cooling demand of the building is registered with a frequency of 1 minute so, after the synchronization process - represented by the 2 columns in the right - each point represents the accumulated capacity of 15 registers of the considered variable and thus, represented in kW/15min. This process is applied to every used variable so that each one has the same timestamp and thus, is synchronized.

4.2.2 Modeling

After the synchronization process, each variable is ready to be modeled. This task demanded the use of a training and prediction algorithm (Adaptive Neuro-Fuzzy Inference System - ANFIS) to calculate the future energy demand of the building which is described in the following section.

4.2.2.1 ANFIS [19] [24] [18]

ANFIS is an algorithm that benefits from the combination of Artificial Neural Networks (ANN's) and a Fuzzy Inference System (FIS). While the ANN's allows the formation of a linguistic rule base, the learning capability of FIS complements the first one drawback, making ANFIS more efficient. This hybrid learning algorithm was firstly introduced in the early 90's by Roger Jang, overcoming the flaws of other modeling systems. This technique provides a method that learns the behaviour of a variable by analysing its values creating correlations with its training inputs. The fuzzy rules have a form of "if-then" rules and define how the output must be for a specific value of membership of its inputs.
The following figure represents a general architecture of ANFIS.

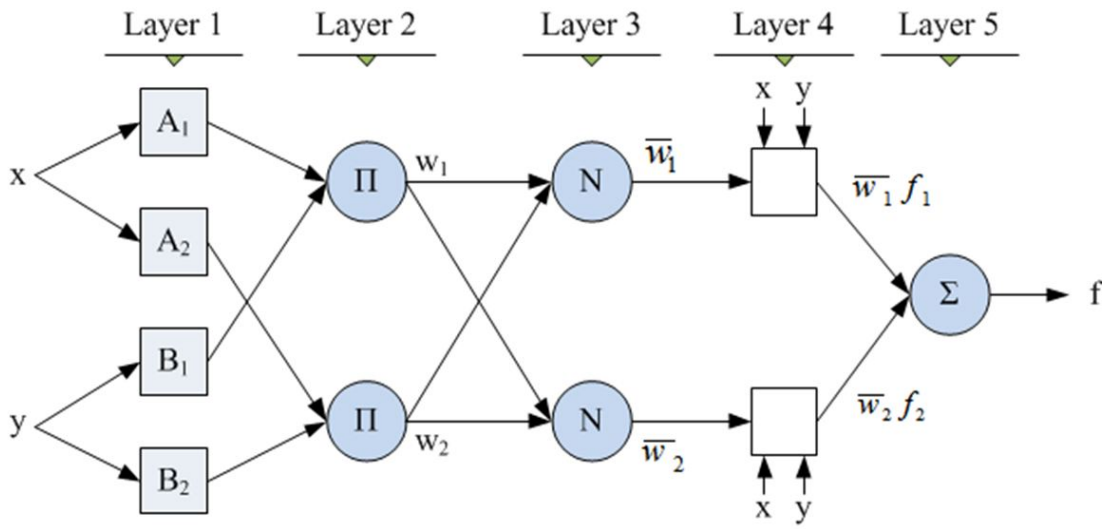

Figure 4.1: ANFIS architecture with two inputs, two rules and one output.

ANFIS is consisted in five layers. The first step is the *fuzzification* process, where each input is converted into membership values (or grade) between 0 and 1 by the membership functions (MF). Equation 4.1 represents the relation between the input and the output of this layer.

$$O_{ij}^{1} = \mu_{ij}(I_i) \tag{4.1}$$

Where O_{ij}^{1} is the output of the j^{th} neuron (A and B in the figure) connected to the i^{th} input, μ_{ij} is the membership function of the input I_i, represented in Figure 4.1 as x and y. Due to its smoothness and concision, the chosen membership function was a Gaussian MF. Its equation is represented bellow.

$$f(x;\sigma,c) = e^{\frac{-(x-c)^2)}{2\sigma^2}} \tag{4.2}$$

Equation 4.2 is specified by the parameters c and σ which represent its center and width and are referred to premise parameters in this layer and they fixed. Figure 4.2 represents the plotting of a general Gaussian MF.

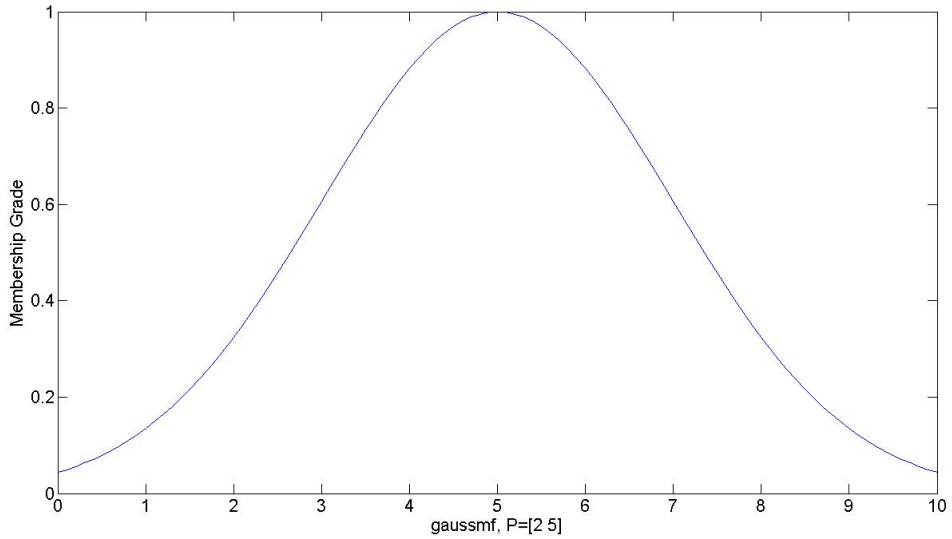

Figure 4.2: Example of Gaussian MF defined by Gaussian(x;5;2).

A general Gaussian curve is observable, where the y axis represents the membership grade. In the second layer, the calculations will determine the strength of each fuzzy rule by multiplying its incoming signals, as represented by the following equation.

$$O_k^2 = \prod(O_{ij}^1) \tag{4.3}$$

In the third layer, a normalization process is made that determines the rule's firing power. A higher value means that the rule influence the decision of the final output. Each calculated firing power has a number between 0 and 1 and collectively sum to 1. This process is calculated by the division of every firing power by the sum of all the firing powers from the second layer. This process is presented in the following equation.

$$O_i^3 = w_i = \frac{O_i^2}{\sum_j O_j^2} \tag{4.4}$$

Where O_i^3 is the output of this layer.
In layer 4, a *defuzzification* process occur that calculates the output for each rule. The output of this layer represents a weighted sum of the original inputs given to the system (I_j is represented in

Figure 4.1 by x and y in Layer 4 and, together with b_j, represent the parameter set), multiplied by the weights given in layer 3 (O_i^3). Equation 4.5 presents this process.

$$O_i^4 = w_i f_i = w_i(\sum_j p_j I_j + b_j) \tag{4.5}$$

The parameters of this layer are known as consequent parameters and they are estimated by the algorithm.
Finally, in the fifth layer, the output is obtained as a sum of the outputs of the previous layer, represented by Equation 4.6.

$$O_i^5 = \sum_j O_j^4 \tag{4.6}$$

The following section describes the aplication of this predictive algorithm in this project.

4.2.2.2 Predicting Models

As described in Section 4.2.2.1, one of the biggest advantage of ANFIS is the capability of learning the behaviour of a variable by creating correlations with its training inputs. These training inputs are referred to as energy drivers and are the variables that affect the operation of the consumption. In this project, the drivers considered were the climatic data (outside temperature and the solar radiation), the minute of the day, the day of the week and the historic consumption of the past 1 day, 2 days, 1 week and 2 weeks. From the eight presented drivers, the last six drivers are called booleans [1] and they take the value 0 or 1, i.e., if they are activated and thus, used as inputs, or not. If they are activated, they will be introduced as a vector with equal size of the vector that wants to be predicted. In the other hand, the consumption reference of each model is referred to as target. ANFIS is applied for each predicted point so, if the prediction is made for a 100 point target, ANFIS will be runned 100 times.

A study was made to each consumption to determine what was the best combination of booleans that indicated which ones were used during the training. The best combination was determined by the calculation of the RMSE, represented bellow by Equation 4.7.

$$\sqrt{\frac{1}{n}\sum_{i=1}^{n}(r_i - p_i)^2} \tag{4.7}$$

[1] On algebra, booleans are the variables that are true or false, i.e., 0 or 1. This term was firstly introduced on 1913 by Henry M. Sheffer. [10]

Where r_i representes the real values and p_i the predicted one.
As its names suggests, the Root Mean Square Error stands for the root of the mean of the square at each point where r and p represents the real consumption values and the predicted values respectively. In the other way, to convert the RMSE values into %, the RMSE value must be divided with the maximum value of the corresponding target. This conversion is represented in Equation 4.8.

$$RMSE\% = \frac{RMSE}{max(target)} \tag{4.8}$$

The following figure presents the structure of the Matlab function which trains its mathematical model and stores it to a "mat" file, which are binary MATLAB format files that store workspace variables[2].

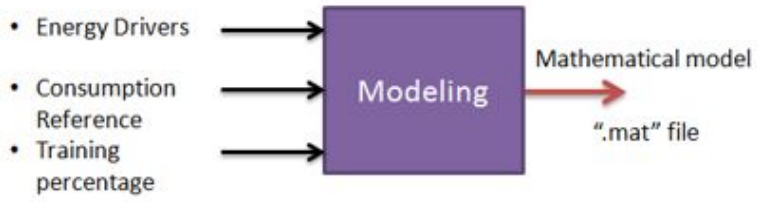

Figure 4.3: Block diagram with the modeling structure.

On the left of the figure are represented the selected energy drivers that changes for each model, the consumption reference or target and the training percentage that determines the amount of data used for training and validation. In Statistics, for modeling validation, it is determined an amount of data used for training and validation. The first one estimates the performance of different models to choose the best one and the second one, having chosen the final model, it estimates its predicting error.
The function created to model the data has the following MATLAB structure: [Result]= Modelingfunction(*EnergyDrivers*, *ConsumptionRef*, *TrainingPerc*). Table 4.2 describes the components of the modeling function.

[2] http://www.mathworks.com/help/matlab/import_export/view-the-contents-of-a-mat-file.html

Table 4.2: Description of the different components of the modeling function.

Inputs/Outputs	Size	Description
EnergyDrivers	MxN	It is a matrix of M rows and N columns which contains the training inputs for the modeling. These data are the variables that affect the operation of the consumption.
ConsumptionRef	Mx1	It is a vector which contains the energy consumption data of the load that is being modeled (reference).
TrainingPerc	1x1	It is a percentage value which defines the splitting proportion of data to be used for training and validation. It takes values between 0 and 1. It was used the value 0,7. That means that 70% of the data is used for the training and the remaining 30% are used for validation.
Result	1x1	It is the model of the consumption, expressed as a Matlab Structure.

4.3 Characterization of the Equipment

The purpose of this section is to define the efficiency of each considered equipment. The resulting equation that defines it allows the determination of its value at any moment if the considered variables are known. These equations were determined through a multiple linear regression analysis. As can be seen in Figure 3.6, the equipment that take part of the building are the solar thermal panels, the boiler, the chiller and the air handling units, however, the last ones weren't considered for this section.
Statistically, a multiple linear regression is a predictive analysis that allows the comprehension of the relationship between one continuous dependent variable and two or more independent variables. Equation 4.9 represents the general model for multiple linear regression.

$$y = \beta_0 + \beta_1 . x_{i1} + \beta_2 . x_{i2} + ... \beta_p . x_{ip} \tag{4.9}$$

Equation 4.9 is valid for i=1...n. The determination of the dependent variable y is influenced by the independent variables x_{ip} and the objective of the regression analysis is to determine the coefficients β. Table 4.3 describes the dependent and independent variables that were considered for the determination of each efficiency.

Table 4.3: Dependent and independent variabels considered in the equipment efficiency determination.

	Chiller	Boiler	Solar Panels
Dependent Variable	COP	Boiler Performance	Panels Performance
Independent Variables	- Outside Temperature - Setpoint Temperature	- Heating Total Demand - Outside Temperature	- Outside Temperature

The dependent variables that were considered for the determination of the effiency of the chiller, the boiler and the solar panels were the Coefficient of Performance (COP), the boiler

performance and the panels performance, respectively. By definition, COP is the measure of power input into the system compared to the power output. Analysing Figure 3.6, for the chiller, the input is the electrical total power and the output is the cooling total power. The same process is applied to the other equipment. As so, for the boiler, the input is total gas power and the output is the heating total power and for the solar panels, the input is the solar radiation and the output is the thermal solar power. Equations 4.10, 4.11 and 4.12 represent these three coefficients.

$$COP = \frac{CoolingTotalPower}{ElectricalTotalPower} \tag{4.10}$$

$$BoilerPerformance = \frac{HeatingTotalPower}{GasTotalPower} \tag{4.11}$$

$$PanelsPerformance = \frac{ThermalSolarPower}{SolarRadiation} \tag{4.12}$$

4.4 Mathematical Formulation of the System

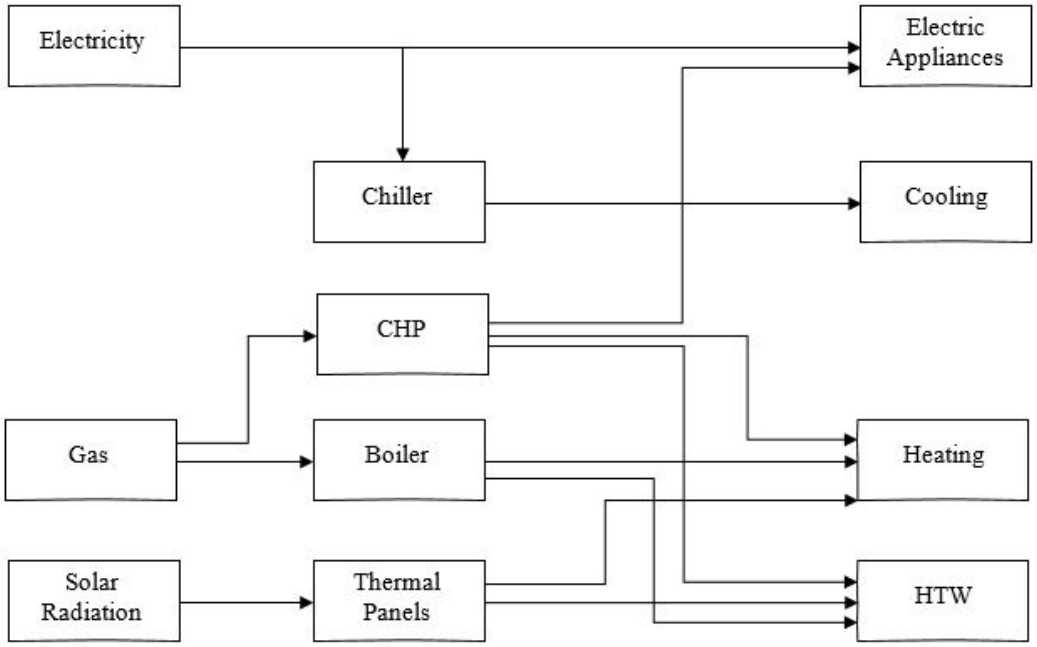

Figure 4.4: Energy hub structure of the building.

In Sections 4.3 and 4.2.2.2, the equipment's coefficients of performance and the building's demands were characterized, thus, this section presents the equations that determine the flow from the inputs to the outputs.
Equation 4.13 represents a coupling matrix that describes the transformation of the energy from the suppliers to the demands where the left matrix corresponds to the different energy demands, the middle matrix to the different equipment's effiency and the right matrix to the different sources of energy.

$$\begin{bmatrix} L_\alpha \\ L_\beta \\ \vdots \\ L_\psi \end{bmatrix} = \begin{bmatrix} \eta_{\alpha\alpha} & \eta_{\beta\beta} & \cdots & \eta_{\omega\alpha} \\ \eta_{\alpha\beta} & \eta_{\beta\alpha} & \cdots & \eta_{\omega\beta} \\ \vdots & \vdots & \ddots & \eta \\ \eta_{\alpha\psi} & \eta_{\beta\psi} & \cdots & \eta_{\psi\omega} \end{bmatrix} * \begin{bmatrix} P_\alpha \\ P_\beta \\ \vdots \\ P_\psi \end{bmatrix} \tag{4.13}$$

From this general equation it is possible to define the energy hub of the building (Equation 4.9), describing the connections between the energy demand vectors (L) and the primary energy sources (P) through the equipment's coefficients of performance (η). As can be seen in Figure 4.4, the hub includes three energy sources - electricity from the grid, natural gas from the network and solar radiation converted to heat through the thermal panels - and four energy demands - electricity, heating, cooling and HTW (not included in this task). There's also a Cogeneration / Combined Heat and Power (CHP) equipment that produces heat and electricity, a chiller, a boiler and thermal panels. The vectors that result from this equation are called equality constraints.

$$\begin{bmatrix} L_{Elec} \\ L_{Heat} \\ L_{Cool} \end{bmatrix} = \begin{bmatrix} 1 & \eta_{electCHP} & 0 & 0 & 0 \\ 0 & \eta_{gasCHP} & \eta_{Boiler} & 1 & 0 \\ 0 & 0 & 0 & 0 & \eta_{Chiller} \end{bmatrix} * \begin{bmatrix} P_{Elec} \\ P_{CHP} \\ P_{Boiler} \\ P_{Solar} \\ P_{Chiller} \end{bmatrix} \tag{4.14}$$

The second step to define the energy hub is to represent the system's restrictions (inequality constraints) that are limitations of energy supplying to the plant and usage of the equipment as represented in Equation 4.15.

$$P_{CHP} + P_{Boiler} \leq P_{gasNetwork} \tag{4.15}$$

Equation 4.14 expresses the limitation of the consumption of gas from the network. The sum of the gas consumed by the boiler and the cogenerator has to be smaller or equal to the supply of gas by the network. To complete the characterization of the system, the vectors with operation limits of the equipment are generated, as described in the following equation.

$$\begin{bmatrix} 0 \\ P_{CHP}^{min} \\ P_{Boiler}^{min} \\ P_{Solar}^{min} \\ P_{Chiller}^{min} \end{bmatrix} \leq \begin{bmatrix} P_{Elec} \\ P_{CHP} \\ P_{Boiler} \\ P_{Solar} \\ P_{Chiller} \end{bmatrix} \leq \begin{bmatrix} P_{elect}^{grid} \\ P_{CHP}^{max} \\ P_{Boiler}^{max} \\ P_{Solar}^{max} \\ P_{Chiller}^{max} \end{bmatrix} \tag{4.16}$$

Equation 4.16 defines, as can be seen, the operating limits of the equipment.
The next section will describe the different steps of the optimization process.

4.5 Optimization

This section purpose was optimizing the energy flow in the system's energy hub using a predicting and an optimization algorithm - ANFIS and Sequential Quadratic Programming (SQP) - for a 24 hour period with the aim of satisfying different optimization criteria. As so, minimization of the total primary energy use, minimization of the CO_2 emissions and minimization of the total energy cost.
The optimization process sets the minimization of a fitness function (Equation 4.12) under a set of inequality and equality constraints and operating bounds, described in the previous section. The fitness function is defined by the summation of each criteria with different weights and it is represented in Equation 4.17.

$$ff = (\sum_{i=1}^{\alpha} p_i.K_i^{en}).w_1.n_1 + (\sum_{i=1}^{\alpha} p_i).w_2.n_2 + (\sum_{i=1}^{\alpha} p_i.f_i).w_3.n_3 \tag{4.17}$$

Where α is the number of primary energy sources, p is the total use of primary energies which is calculated by the SQP, K^{en} corresponds to the prices of the primary energy sources, f is the emission factor, w are the weight factors given to each criterion and n are the constants for the per unit transformation of each criterion. The SQP generates iterations that converge to a solution of a problem by solving quadratic programs. The optimization problem that is set to be solved is represented as follows.

$$\begin{gathered} \text{Minimize} \\ ff \\ \text{Subject to:} \\ \eta.P = L \\ A.P \leq b \\ l_b \leq P.\eta \leq u_b \end{gathered}$$

The three equations that the fitness function is subjected to, correspond to the equality and inequality constraints and the operating bounds represented in Equations 4.14, 4.15 and 4.16.

Chapter 5

Results and Discussion

5.1 Inputs

In this Section are presented the considered inputs of the building that were used to model the different demands, as well as its graphic representation with the percentage of data used in training and in validation. All the data was downloaded considering the period from the 3rd of November of 2014 to the 3rd of November of 2015.
After the synchronization process described in Section 4.2.1, every considered demand was ready to be modelled as the meteorological data was synchronized in time with each demand.
Figures 5.1 and 5.2 represents the two meteorological data that were used during the training and validation process of ANFIS.

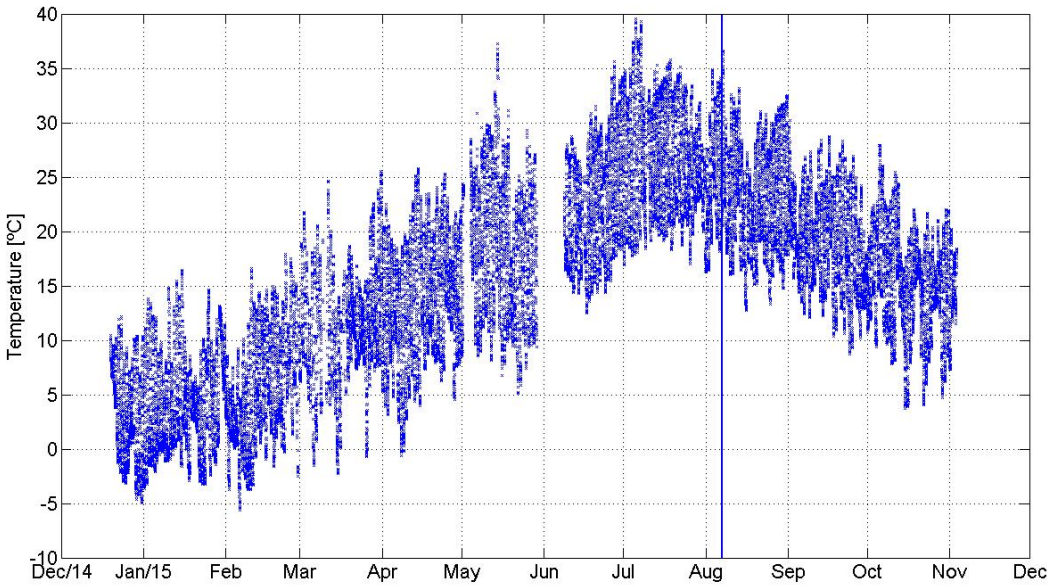

Figure 5.1: External temperature.

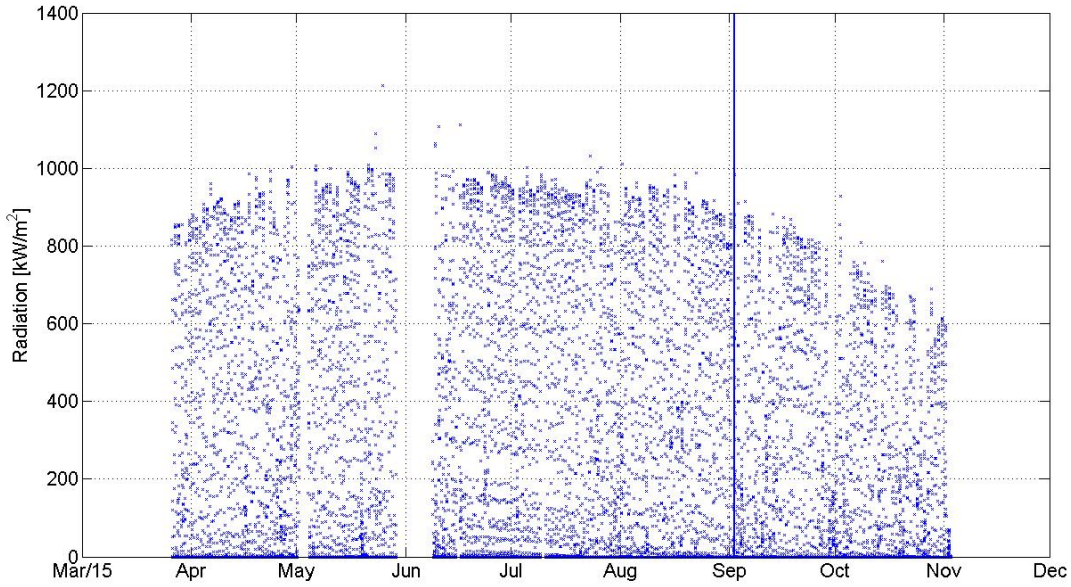

Figure 5.2: Solar radiation.

As can be observed, the line marks the separation of data that was used for training (70%) and for validation (30%) when used on ANFIS. Also, despite the fact that the data was downloaded from November 2014 till November 2015, as can be seen for both data, it does not begin on November 2014. That fact occurs because the meteorological station of CTM only started recording the external temperature in the end of December 2014 and solar radiation in the end of March 2015. Furthermore, as expected, the temperature increases till it reaches its peack on July/August. At this time, the line that determines the start of the data used for validation is set, that allows all the range of temperatures for training and validation. Something similar happens with solar radiation where it reaches its peack during July and August and the data used for validation starts on September that allows all range of values for both processes as well. Additionally, the 'holes' in the data observed in the beggining of July for the external temperature and in the end of May and beggining of June for the solar radiation, represents periods where the meteorological station didn't recorded that specific data.

The following table represents specific information about the meteorological data used for modeling.

Table 5.1: Specific information about the training and validation processes for both meteorological data used for modeling.

		Solar Radiation [kW/m^2]	External Temperature [^{o}C]
Training	Max	1212.5	39.5
	Min	0	-5.61
Validation	Max	982.9	36.6
	Min	0	3.76

Figures 5.3, 5.4, 5.5, 5.9 and 5.10 represent the three variables that were considered for the characterization of the cooling demand of the building: the total, the AHU and the fan coil consumption in the considered period.

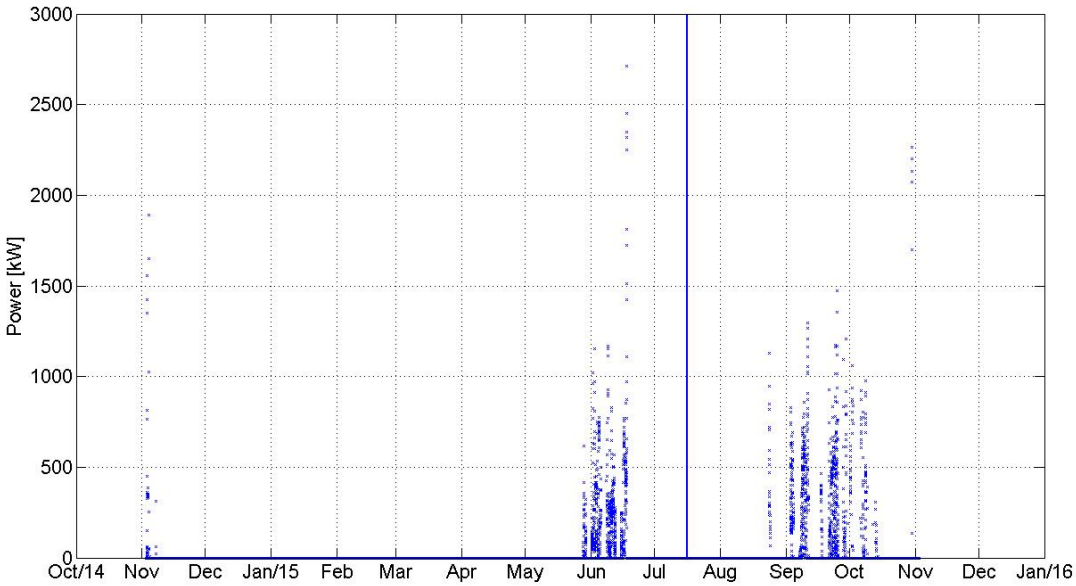

Figure 5.3: AHU cooling demand.

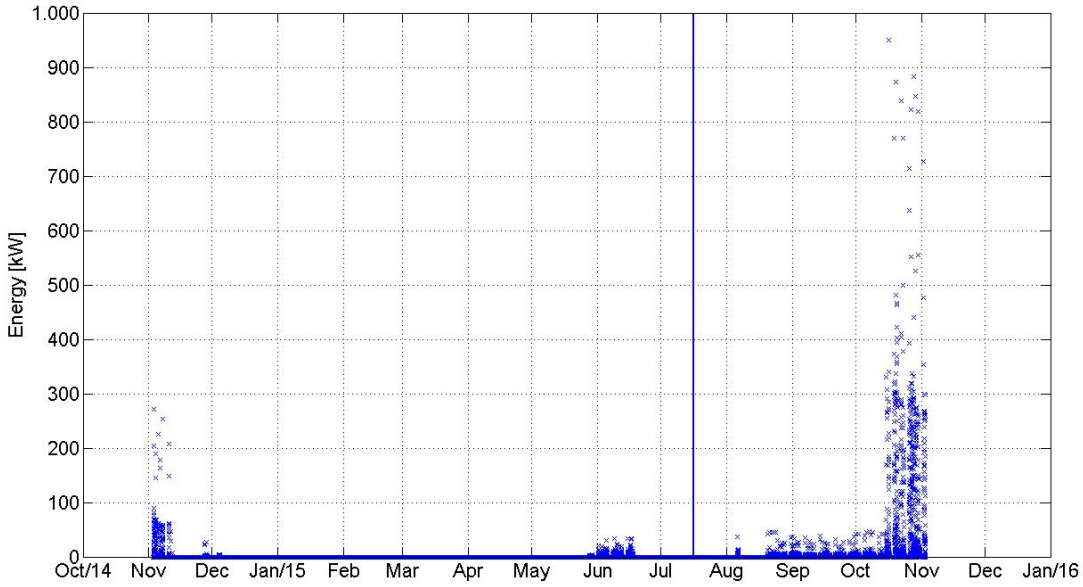

Figure 5.4: Fan coil cooling demand.

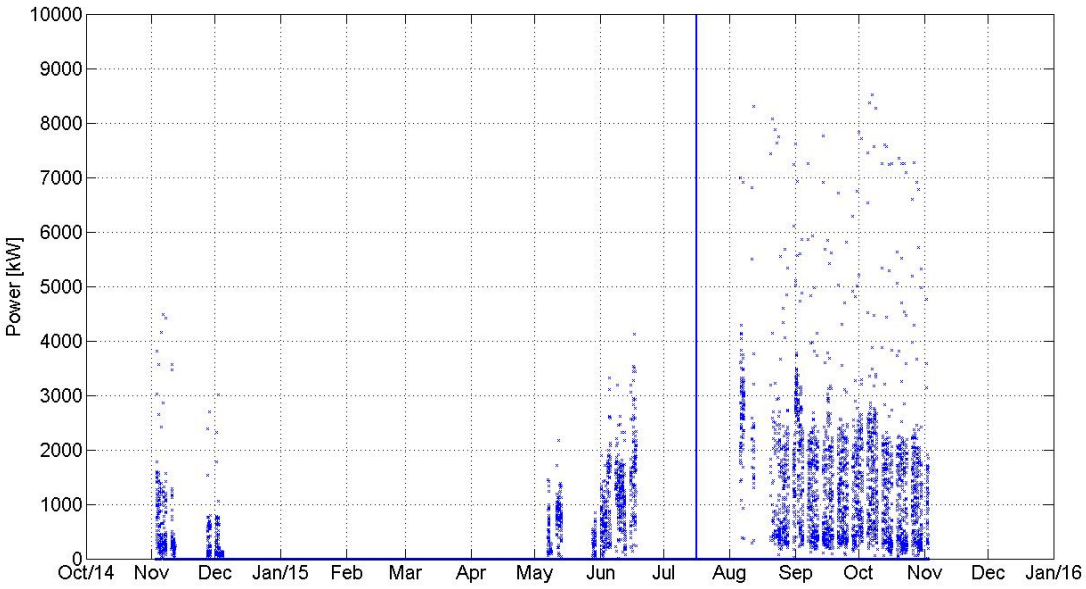

Figure 5.5: Total cooling demand.

Similarly, to characterize the heating necessities, were considered the total, the AHU, the fan coil and the HTW demand. Figures 5.6, 5.7, 5.8 and 5.9 represent these variables.

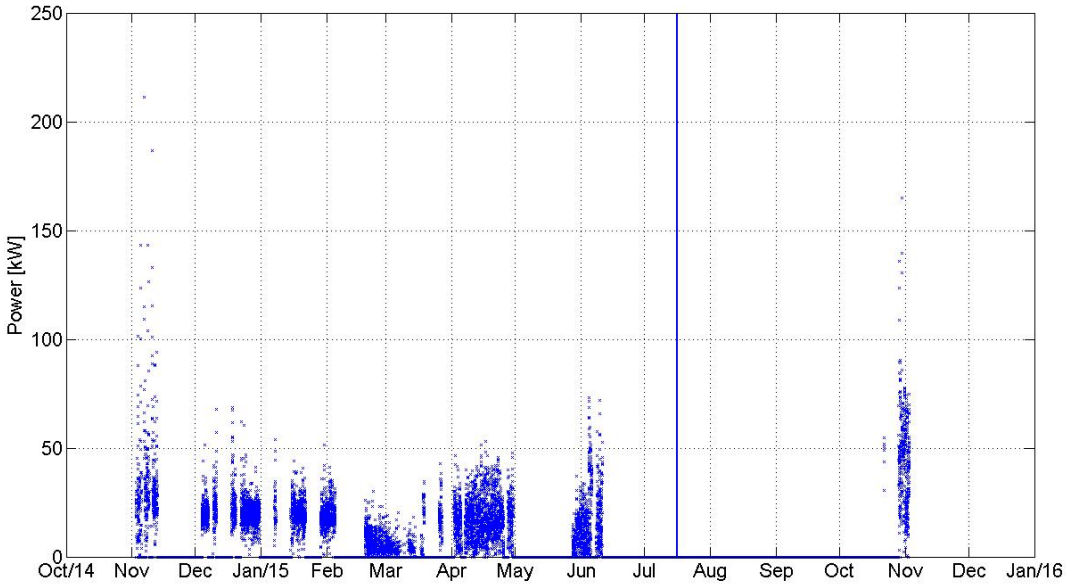

Figure 5.6: AHU heating demand.

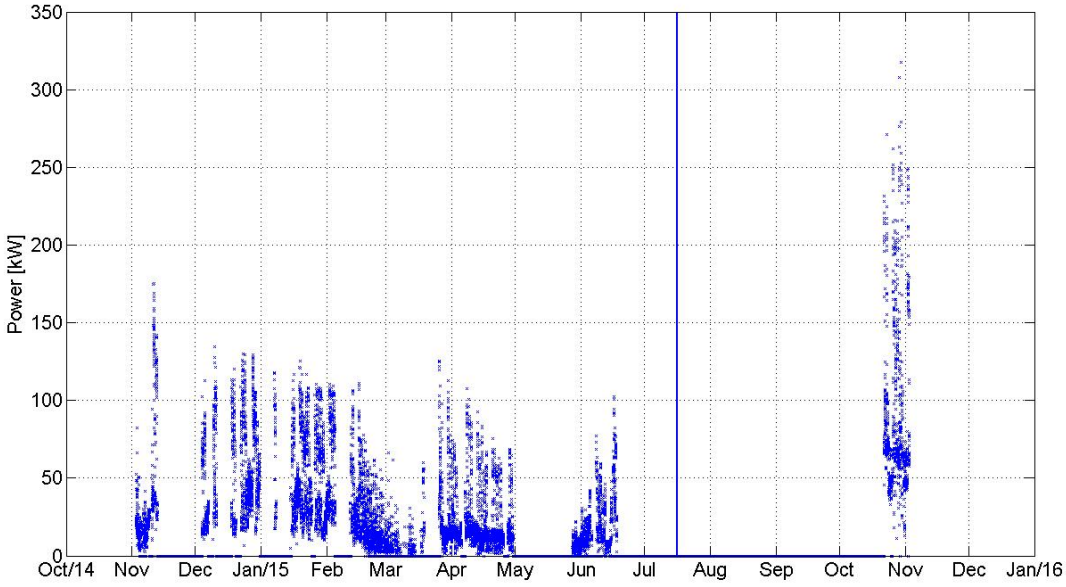

Figure 5.7: Fan coil heating demand.

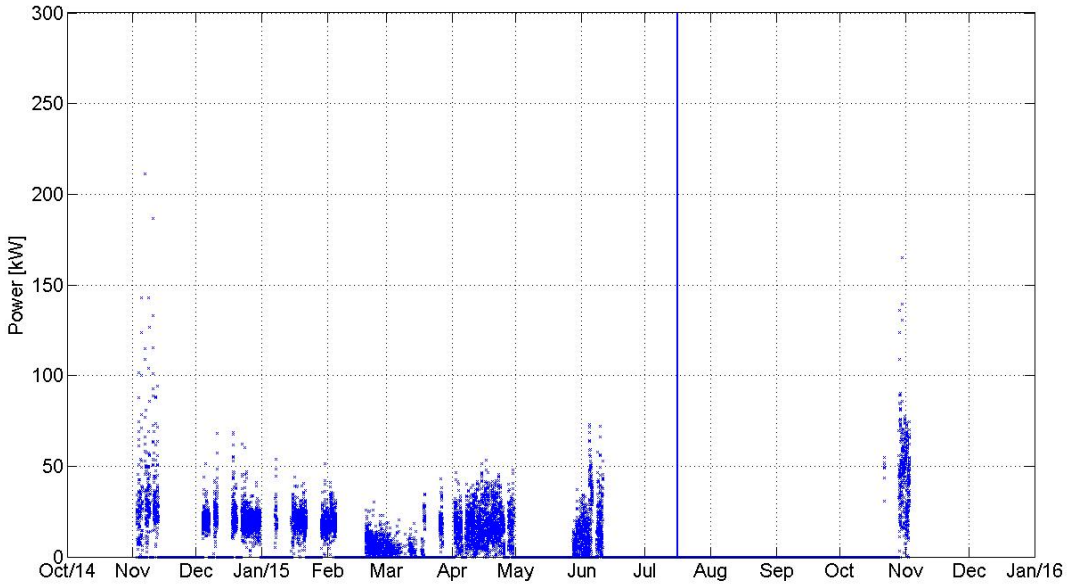

Figure 5.8: HTW heating demand.

As can be seen in the Figure 5.8, the consumption of HTW between the middle of June and the end of October is zero. This could reflect the fact that the HTW is mainly used in the showers of the building so, during the hot days in the Summer, people don't use them. Besides that, during almost all August, the CTM building is closed.

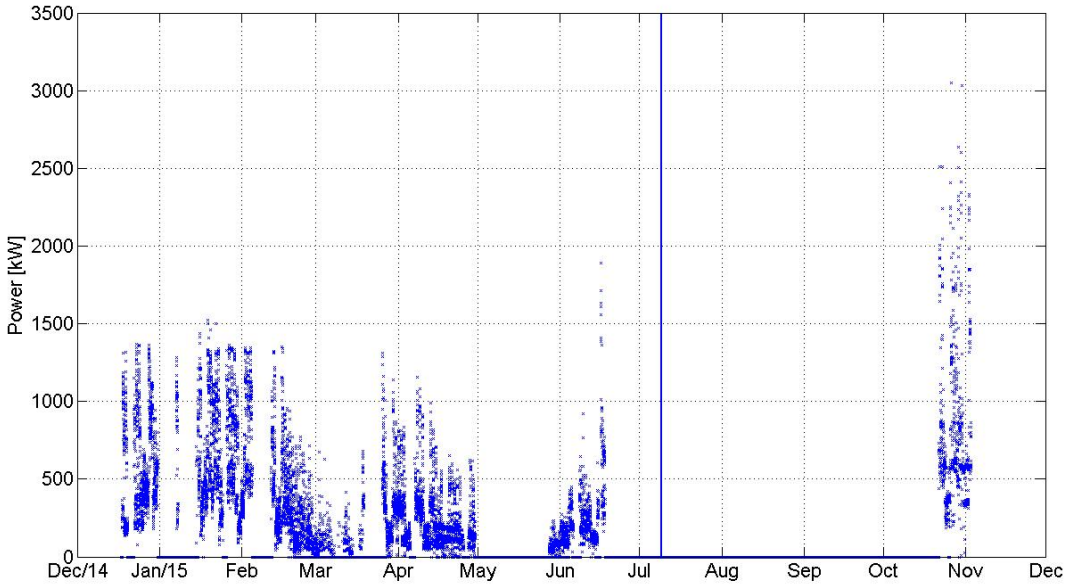

Figure 5.9: Total heating demand.

Finally, for the electric consumption of the building, it was considered the total electric consumption of the building. Figure 5.10 represents the consumption during the considered period.

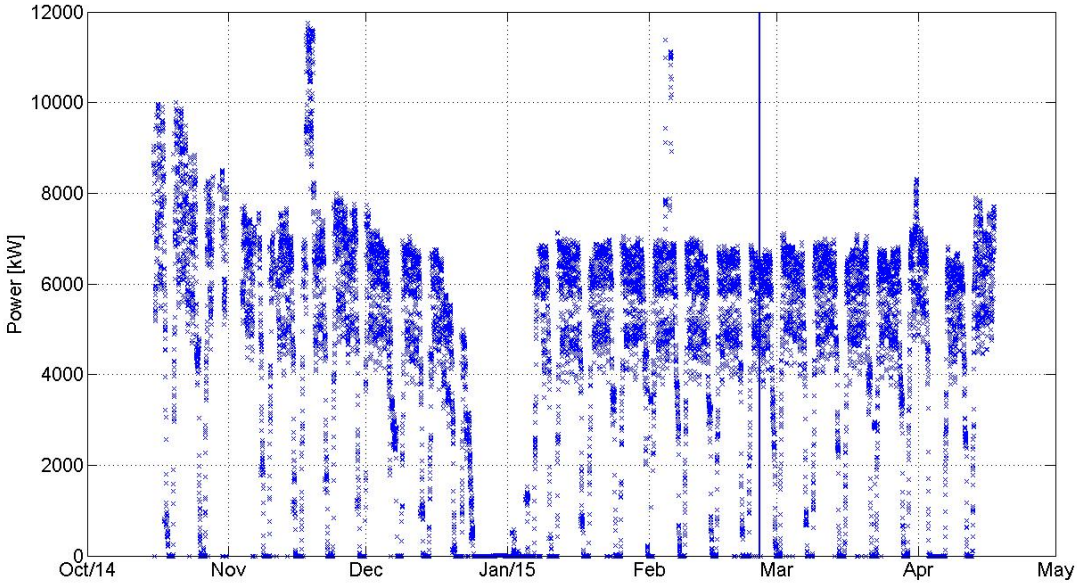

Figure 5.10: Total electrical demand.

Overall, as expected, the heating demand is higher on Winter time and the cooling demand,

roughly, remains constant over the year. Table 5.2 represents the mean and the maximum values for the training and the validation process for the 8 considered variables used to characterize the demands of the building.

Table 5.2: Specific information of the variables used for the modeling process.

Variables [kW]	Training		Validation	
	Max	Mean	Max	Mean
AHU Cooling	$2.71*10^3$	8.69	$2.11*10^2$	1.84
Fan Coil Cooling	$2.72*10^2$	0.433	$9.50*10^2$	8.42
Total Cooling	$4.48*10^3$	45.3	$8.52*10^3$	$3.90*10^2$
AHU Heating	$2.11*10^2$	4.04	$1.65*10^2$	1.84
Fan Coil Heating	$1.75*10^2$	13.2	$3.18*10^2$	9.64
HTW Heating	$4.39*10^2$	18.2	$1.39*10^3$	6.01
Total Heating	$1.89*10^3$	$19.0*10^2$	$3.05*10^3$	80.0
Total Electrical	$1.18*10^4$	$4.03*10^3$	$8.31*10^3$	$4.30*10^3$

As can be seen, the mean values differ their order of magnitude in some cases. This variation can be explained by the lack of registration of heating variables in the end of Summer and Autumn, which has impacts in the validation process. On the contrary, there are some deficiencies on the registration of cooling variables during Spring and the beggining of Summer that affect the training process.
The following table represents the number of data used in the training and in the validation process, as well as its total.

Table 5.3: Number of data used in the training and in the validation process.

Demand Variables	Training	Validation	Total
AHU Cooling	24528	10512	35040
Fan Coil Cooling	24528	10512	35040
Total Cooling	24528	10512	35040
AHU Heating	24527	10512	35039
Fan Coil Heating	24527	10512	35039
HTW Heating	24527	10512	35039
Total Heating	17436	7472	24908
Total Electrical	11390	4882	16272

It is relevant to mention that the negative values are converted to zero as inputs and the holes in the data are not included.

5.2 Modelling

As described in Section 4.2.2, the ANFIS algorithm was used for the modelling process. However, before running ANFIS, its external and internal parameters had to be defined. The external parameters correspond to the inputs selection and the internal parameters to the membership function for each input and the type of membership function for the input and for the output. The internal parameters were defined as default for the first-order of ANFIS. As so: three membership functions for each input; gaussian type for each membership function for the input and linear type for each membership function for the output.
The inputs selection included the meteorological data and the bollean selection. For the meteorological data were considered the external temperature of the building and the solar radiation for every model. For the bollean selection, a study was made to understand which combination was more favourable for each model. ANFIS was runned for each model with every combinations of bolleans for each model and the RMSE was calculated. The best combination of bolleans was the one that created the smaller RMSE.
Table 5.4 represents the best combination of booleans for each variable.

Table 5.4: Best combination of bolleans for each considered variable where: Past 1W refers to the previous week; Past 2W to the previous two weeks; MinDay refers to the minute of the day and DayW refers to the day of the week.

Variables	Past 24h	Past 48h	Past 1W	Past 2W	MinDay	DayW	RMSE %
AHU Cooling Demand	1	1	1	1	1	1	-
Fan Coil Cooling Demand	1	0	1	1	1	1	3.19
Total Cooling Demand	1	0	1	1	1	1	5.80
AHU Heating Demand	1	1	1	1	1	1	-
Fan Coil Heating Demand	1	0	0	0	1	1	4.57
HTW Heating Demand	1	1	1	1	1	1	4.18
Total Heating Demand	1	1	1	1	0	1	5.53
Total Electrical Demand	1	0	1	0	1	1	12.0

If the bollean is 1, then a vector with an equal size of the one that wants to be predict is processed and used as an input. Four of the bolleans correspond to past consumptions, which means that for every predicted point, if the late consumption bolleans are activated, the consumption of that minute is used as an input. The other two bolleans correspond to the day of the week (1 to 7) and the minute of the day (0 for 00:00 to 1435 for 23:45).

Tables 5.4 and 5.5 represent an example of how the activation of the bolleans works for past consumptions (Table 5.5) and for the day of the week and minute of the day (Table 5.6). This examples are made to predict the first 3 hours of the 25th of December of 2014 of a random demand value.

Table 5.5: Example of vectors used as inputs on ANFIS in the prediction of consumption for the first three hours of the 25th of December with the values in kW.

Consumption	(reference)	Consumption	(-1 day)	Consumption	(-1 week)
Time	Value	Time	Value	Time	Value
25-Dez,00:00	228.60	24-Dez,00:00	**246.00**	18-Dez,00:00	**235.08**
25-Dez,00:15	238.60	24-Dez,00:15	**280.04**	18-Dez,00:15	**272.40**
25-Dez,00:30	230.68	24-Dez,00:30	**251.36**	18-Dez,00:30	**257.36**
25-Dez,00:45	243.44	24-Dez,00:45	**246.96**	18-Dez,00:45	**237.72**
25-Dez,01:00	233.48	24-Dez,01:00	**256.60**	18-Dez,01:00	**266.04**
25-Dez,01:15	249.00	24-Dez,01:15	**248.60**	18-Dez,01:15	**249.92**
25-Dez,01:30	240.36	24-Dez,01:30	**251.60**	18-Dez,01:30	**235.04**
25-Dez,01:45	230.68	24-Dez,01:45	**272.64**	18-Dez,01:45	**267.84**
25-Dez,02:00	233.20	24-Dez,02:00	**250.80**	18-Dez,02:00	**254.92**
25-Dez,02:15	236.52	24-Dez,02:15	**259.08**	18-Dez,02:15	**242.16**
25-Dez,02:30	230.24	24-Dez,02:30	**257.72**	18-Dez,02:30	**265.28**
25-Dez,02:45	258.52	24-Dez,02:45	**253.80**	18-Dez,02:45	**263.00**
25-Dez,03:00	231.56	24-Dez,03:00	**253.56**	18-Dez,03:00	**246.76**

Table 5.6: Example of "Minute of the Day" and "Day of the Week" vectors used as inputs in the prediction of the first three hours of a random variable for the 25th of December of 2014.

Time	Day of the Week	Minute of the Day
25-Dez,00:00	**5**	**0**
25-Dez,00:15	**5**	**15**
25-Dez,00:30	**5**	**30**
25-Dez,00:45	**5**	**45**
25-Dez,01:00	**5**	**60**
25-Dez,01:15	**5**	**75**
25-Dez,01:30	**5**	**90**
25-Dez,01:45	**5**	**105**
25-Dez,02:00	**5**	**120**
25-Dez,02:15	**5**	**135**
25-Dez,02:30	**5**	**150**
25-Dez,02:45	**5**	**165**
25-Dez,03:00	**5**	**180**

As observed in Table 5.5, two vectors of past consumptions are used as inputs to predict the consumption for the 25th of December: the consumption one day before and one week before. In Table 5.6, an example of "Minute of the Day" and "Day of the Week" vectors for the same day is given. As the 25th of December was thursday, the corresponding number is 5 and the minute of the day goes from 0 to 180 rather its 00:00 or 03:00. On both Tables, the columns in bold correspond

to those that enter as inputs in ANFIS.

Table 5.7 represents the number of inputs, fuzzy rules and total parameters for each model. Its representations comparing the predictions with the real consumption are presented next.

Table 5.7: Number of inputs and the number of parameters for each model.

	Nr of Inputs	Nr of Premise Params	Nr of Consequent Params	Total Nr of Params
HTW Heating	8	48	27	75
Total Cooling	7	42	24	68
Total Heating	7	42	24	68
Solar Thermal	7	42	24	68
Fancoil Cooling	7	42	24	68
Total Electrical	6	36	21	57
Fancoil Heating	5	30	18	48

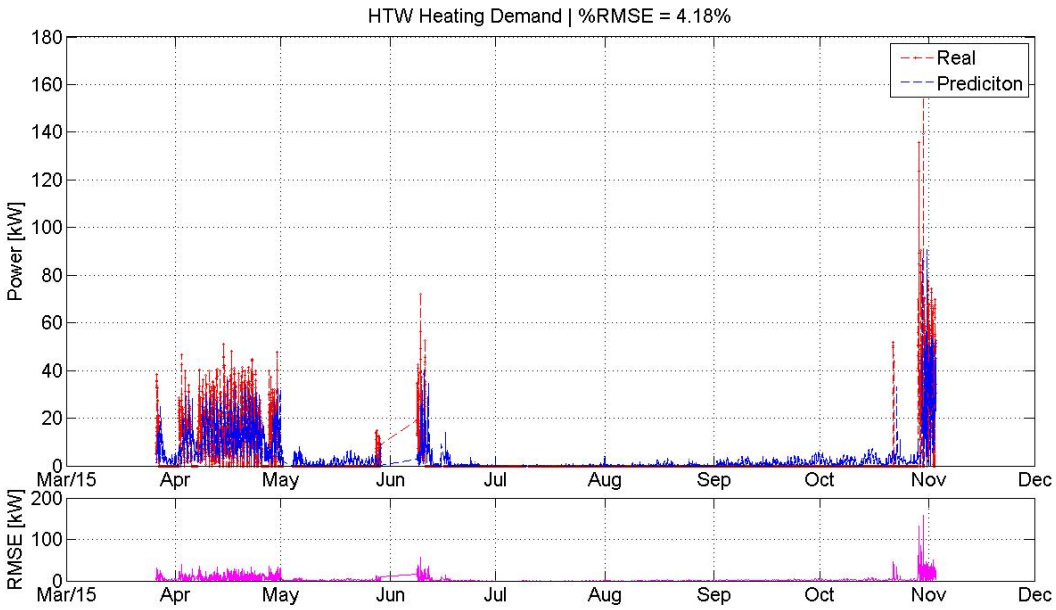

Figure 5.11: Comparison between real consumption and prediction of the HTW heating demand.

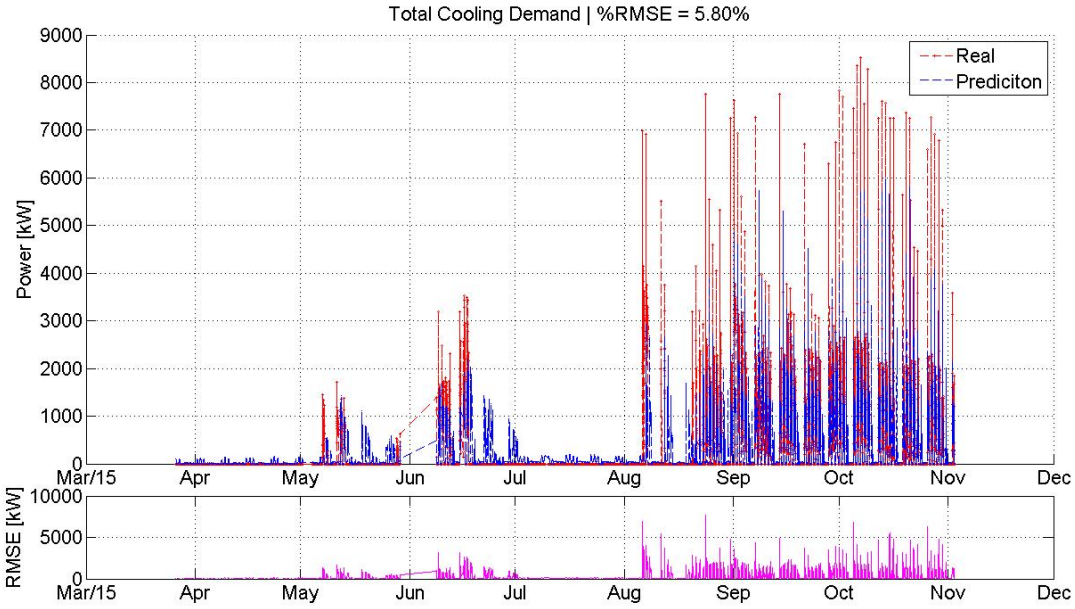

Figure 5.12: Comparison between real consumption and prediction of the total cooling demand.

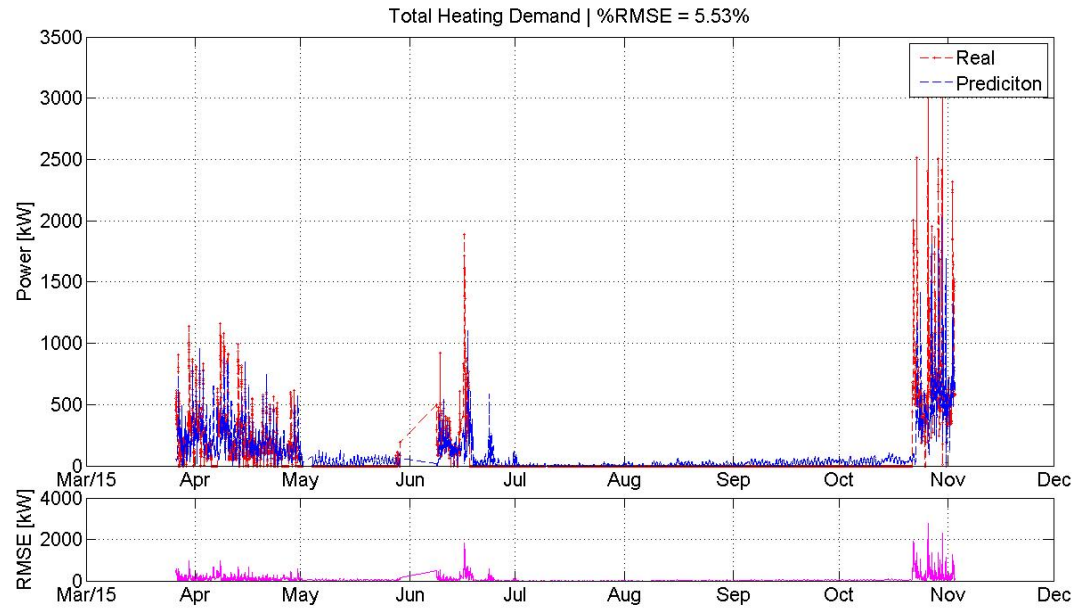

Figure 5.13: Comparison between real consumption and prediction of the total heating demand.

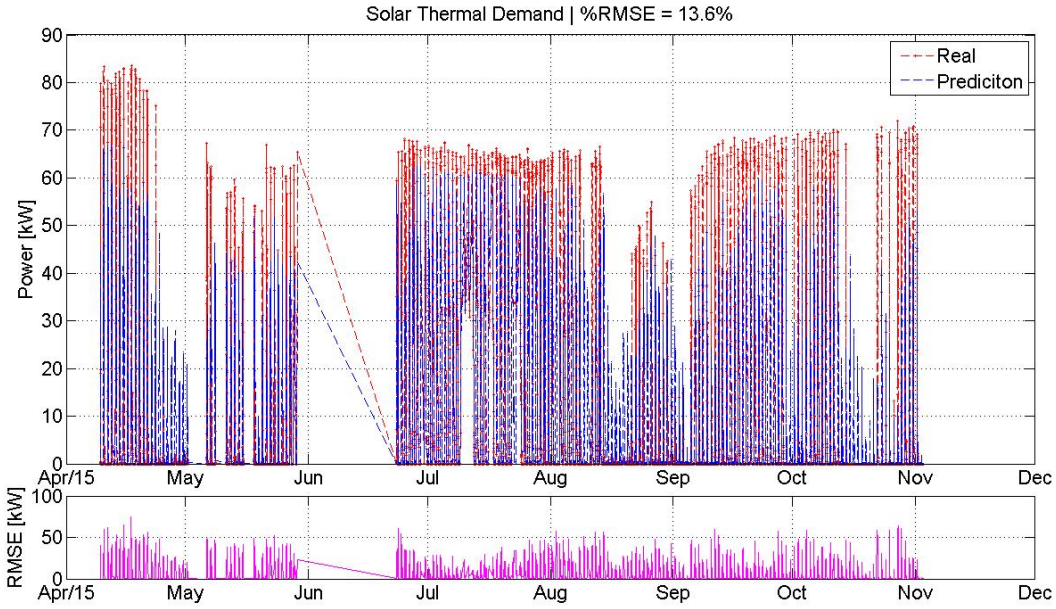

Figure 5.14: Comparison between real consumption and prediction of the solar thermal demand.

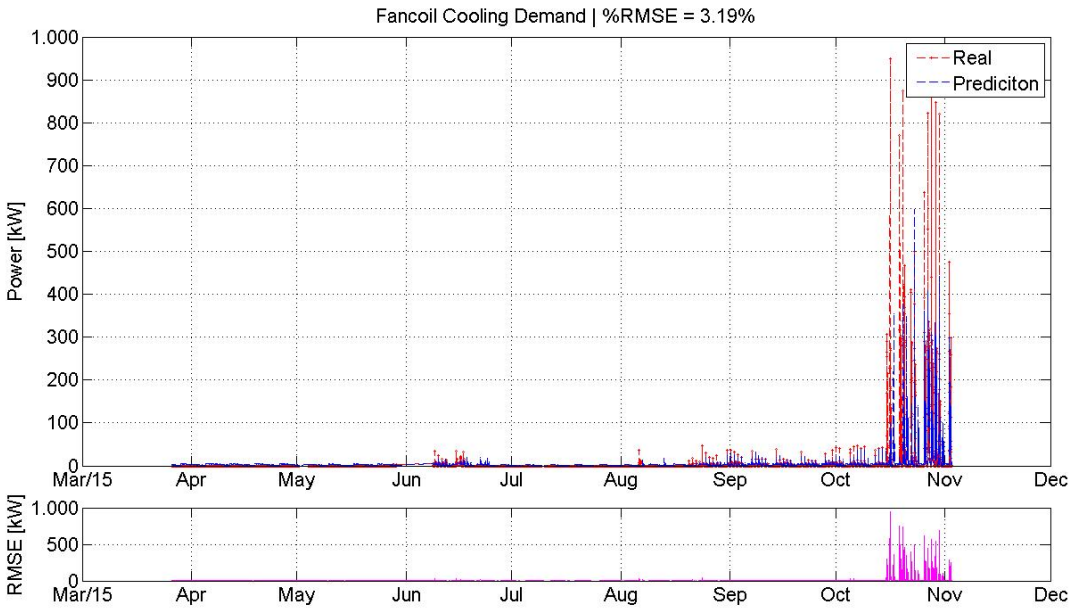

Figure 5.15: Comparison between real consumption and prediction of the fancoil cooling demand.

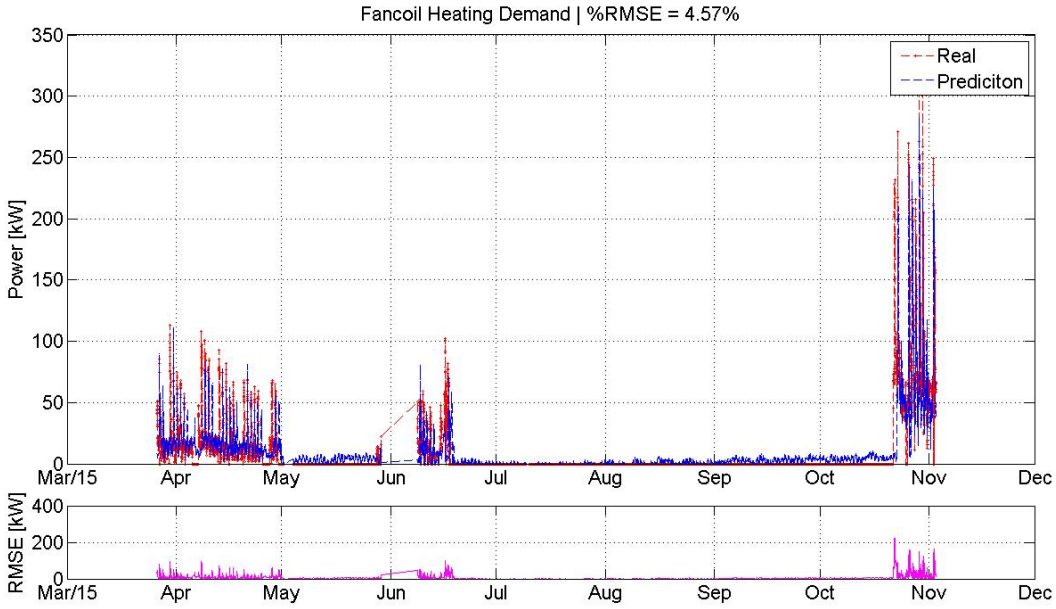

Figure 5.16: Comparison between real consumption and prediction of the fancoil heating demand.

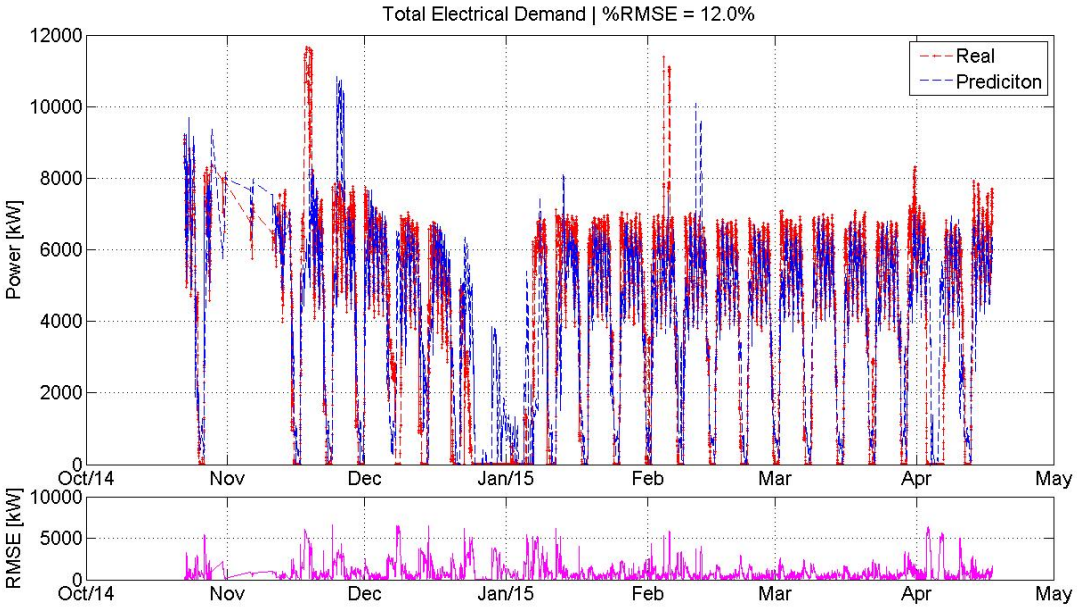

Figure 5.17: Comparison between real consumption and prediction of the total electrical demand.

All models were successfully created with the exception of the models that characterize the AHU heating and cooling demand, that weren't presented in the results.

5.3 Optimization

As described in Section 4.3, after creating the models for each variable the efficiency of the energy's hub equipment had to be defined. The considered equipment were the chiller, the boiler and the combined heat and power cogenerator.
For the chiller, the approach was a multiple linear regression analysis where the independent variable was the Coefficient of Performance and the considered dependent variables were the temperature outside the building and the set point temperature. Each variable suffered a filtration process before the regression analysis. For each variable the *isnan*[1], the *isinf*[2] and zero values weren't considered. Furthermore, the chiller has two pumps functioning so, when the pumps were closed the set point temperature data wasn't considered. An interpolation process was set to overcome the holes in the data that resulted from the filtering process. Figure 5.18 represents the three variables considered after the filtration and interpolation process.

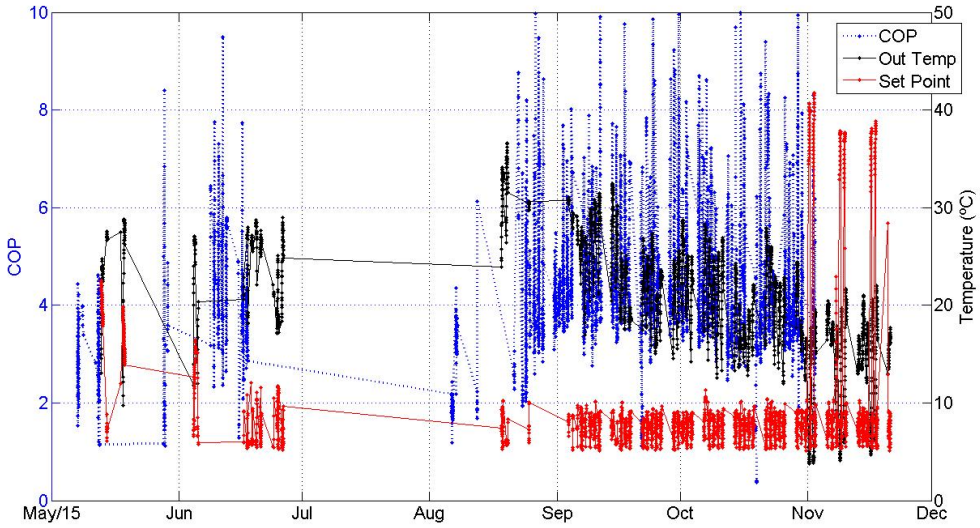

Figure 5.18: Variables considered for the multiple linear regression analysis: set point temperature, COP and temperature outside the building.

As can be seen in the right y-axis, the majority of the set point temperature values are located between 0 and 10ºC and between the end of June and the middle of August there's a huge hole due to the filtration process so, for the multiple linear regression, only some parts of the data were selected.
Equation 4.4 (see Section 4.3) results in Equation 5.1 which represents the equation that defines the chiller's efficiency which results from the multiple linear regression.

[1] Values that are not logical. - http://www.mathworks.com/help/matlab/ref/isnan.html
[2] Values that are infinite. - http://www.mathworks.com/help/matlab/ref/isinf.html

$$ChillerEff = -3.4313 - 4.2952x_1 + 18.5767x_2 - 0.4679x_1x_2 + 0.1463x_1^2 - 0.5126x_2^2 \quad (5.1)$$

The values x_1 and x_2 correspond to the average of the chosen points of the temperature outside the building and the set point temperature in the chiller. The following figure is a 3D graph of the surface that represents the points that result from the linear regression.

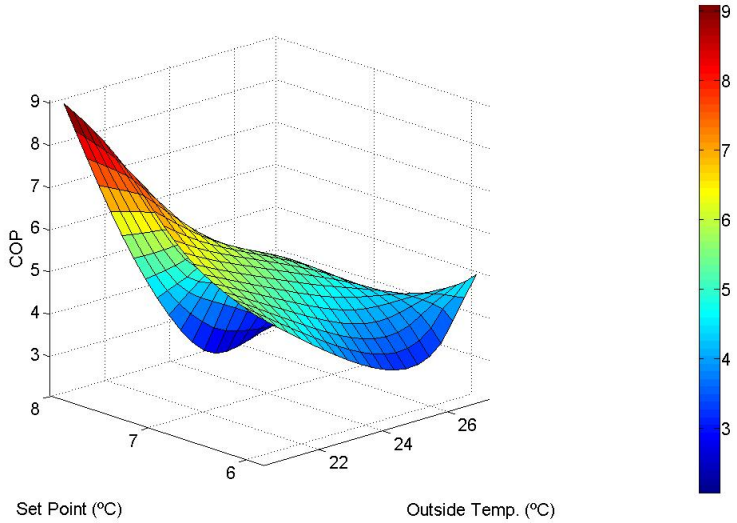

Figure 5.19: Surface representing the efficiency of the chiller considering the temperature outside the building and the set point temperature as dependent variables and the COP as an independent variable.

As can be seen, the efficiency is higher for smaller temperatures of the atmosphere and for higher values of the set point, considering the upper limit of 8°C.
For the other variables were considered values given by CTM. Table 5.8 represents the efficiency values that were used in the optimization process.

Table 5.8: Efficiency values for the CHP, chiller and boiler.

	Electric Cogeneration	Heat Cogenerator	Chiller	Boiler
Efficiency	0.26	0.56	0.36	0.85

The values of the efficiency presented in Table 5.8 are used in Equation 4.9 (described on Section 4.4) to define the carriers of the electricity generation and of heating and cooling production. The resulting equation is presented in Equation 5.2.

$$\begin{bmatrix} L_{Elec} \\ L_{Heat} \\ L_{Cool} \end{bmatrix} = \begin{bmatrix} 1 & 0.26 & 0 & 0 & 0 \\ 0 & 0.56 & 0.85 & 1 & 0 \\ 0 & 0 & 0 & 0 & 0.36 \end{bmatrix} * \begin{bmatrix} P_{Elec} \\ P_{CHP} \\ P_{Boiler} \\ P_{Solar} \\ P_{Chiller} \end{bmatrix} \tag{5.2}$$

In the left matrix in Equation 5.2, the L vaues are substituted for the predictive models presented in section 5.2. For the operating bounds, defined in Equation 4.11 (section 4.4), it was set the value of zero to the lower limit. Multiple scenarios were set for the upper limit and was defined 50000kW for the maximum supply limit of electricity and to the maximum cooling production of the chiller per 15 minute interval and 10000 kW to the maximum supply limit of natural gas, to the thermal production of the cogeneration equipment and to the thermal production of the boiler equipment per 15 minute interval.

To satisfy the optimizing criteria, the prices of electricity and gas had to be defined. The price for the gas was set on 0.068 Eur/kWh[3] and for the electricity 0.14 Eur/kWh [4]. The CO_2 emissions factor of electricity is 0 and of gas is 1.2 kg CO_2/kWh. Both values where given by CTM.

To conclude, the weight of each criteria has to be defined. As three different optimization criteria are considered, there are 6 different combinations. The results were all the same except when it was considered only the cost minimization so, the results presented as follows consider two scenarios. Scenario I represent 5 combinations and scenario II represent the combination when only the cost minimization is considered.

Figure 5.20 represents a comparison between the energy demand (real and predicted) and the production calculated by the algorithm that are equal for both scenarios. The three subplots correspond to the electrical, heating and cooling power. The prediction is made for a 24 hour period.

All the optimization units are presented in pu (per unit) values, which required the division of all the values by its maximum value.

[3] Value defined as an average of the presented values in http://www.galpenergia.com/PT/ProdutosServicos/GasNatural/Mercado-Regulado/Tarifario/Paginas/Tarifario.aspx?tipoUtilizacao=1

[4] Value consulted in http://www.pordata.pt

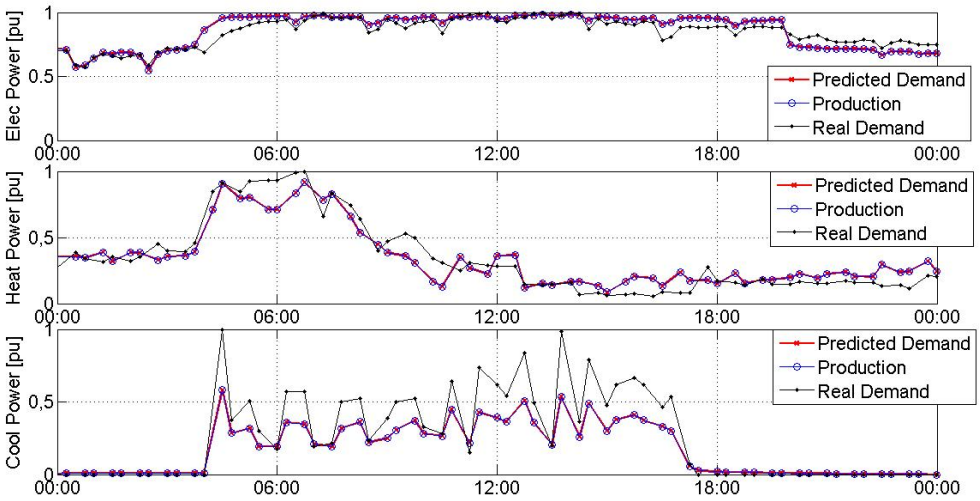

Figure 5.20: Energy demand vs energy production for electric, heating and cooling power.

As observed, the production satisfies the demand for each variable.
Figures 5.21 and 5.22 presents the use of the primary energy sources by each equipment that was necessary to produce the required energy for scenario I and II, respectively.

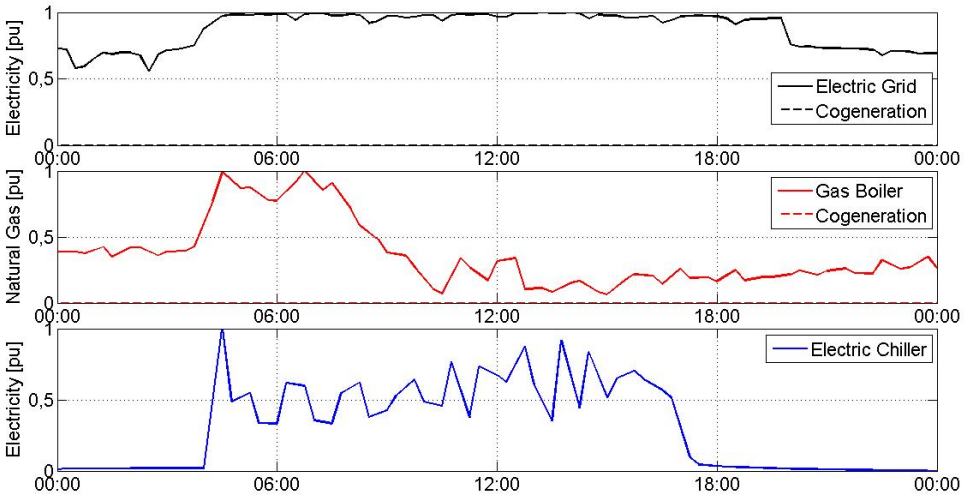

Figure 5.21: Total use of primary energy sources by each equipment for scenario I.

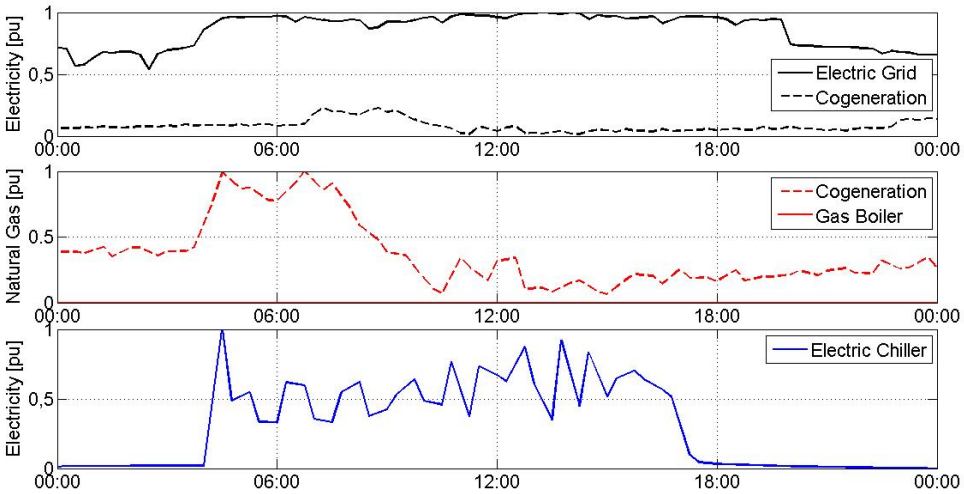

Figure 5.22: Total use of primary energy sources by each equipment for scenario II.

As can be seen, the consumption of electricity by the chiller from the grid is the same in both scenarios. For the total electrical demand, the production of electricity by the cogenerator for scenario I is zero and for scenario II the cogenerator produces some electricity, although the major consumption is still from the grid. On the other hand, the natural gas use is distinct in each scenario. In scenario I, the total use of natural gas comes from the boiler and in scenario II it comes from the CHP. The use of these primary energy sources is presented in the following figure.

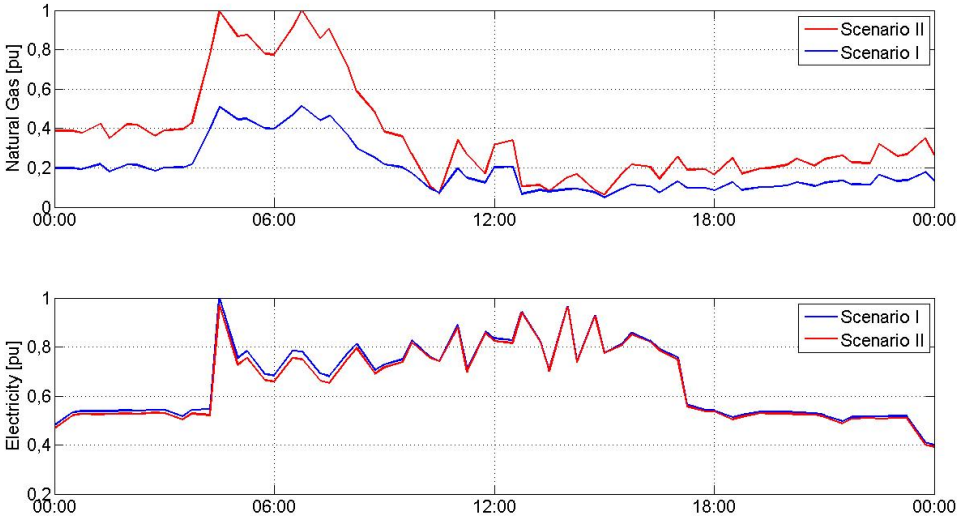

Figure 5.23: Total use of primary energy sources for both scenarios.

As observable, natural gas use on scenario II - where the CHP is responsible for all the production - is much higher than in scenario I when the boiler is responsible for the production. This fact is explainable for the lower efficiency of the CHP (0.56) compared to the efficiency of the boiler (0.85). On the other hand, the electricity use is slightly lower on scenario II, where the CHP produces electricity.
Figure 5.24 represents the costs and emissions for both scenarios.

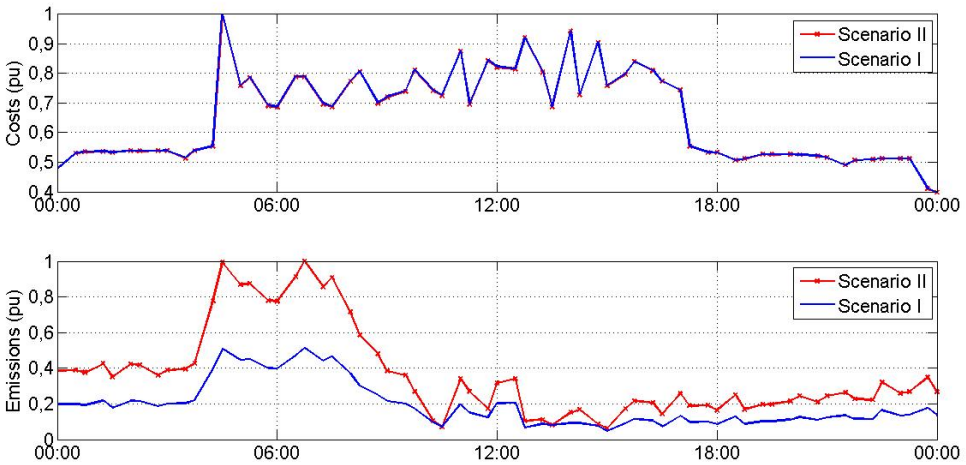

Figure 5.24: Costs and emissions for scenario I and II.

As the costs are the same in both scenarios, the emissons are much higher for scenario II than for scenario I, which is justified for the much higher consumption of natural gas, as can be seen on Figure 5.23.
To overcome the inefficiency of the use of the CHP in the previous scenarios, a new one was created where the efficiency of the cogeneration of heat is 0.85 - Scenario III. In this scenario, the weight of each criteria is the same applied in Scenario II, i.e., only the costs minimization is set for the optimization process.
The following figures compares the total use of primary energy sources and its correspondent costs and emissions for Scenario II and III.

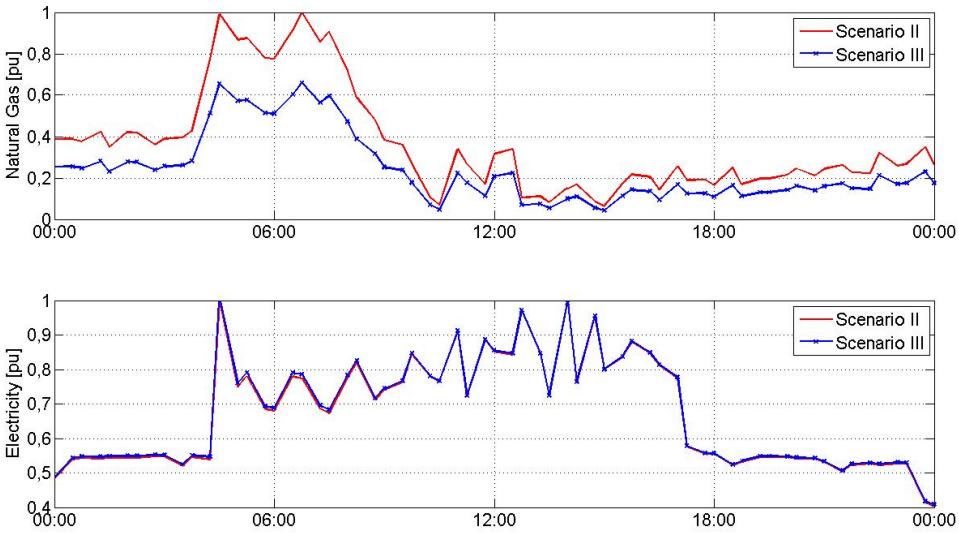

Figure 5.25: Total use of primary energy sources for Scenario II and III.

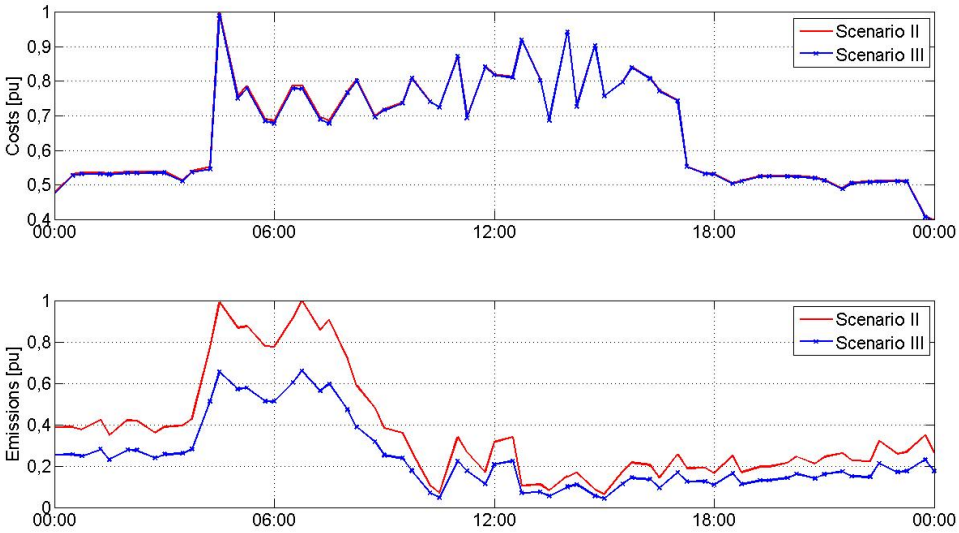

Figure 5.26: Costs and emissions for Scenario II and III.

As expected, Figures 5.25 and 5.26 demonstrate that the natural gas consumption reduces and, consequently, either the emissions. A similar comparison was made with Scenarios III and I, with a similar profile of Figures 5.21 and 5.22 where the heat production comes totally from cogeneration in Scenario III and from the boiler in Scenario II. Although, the electrical production in Scenario III in lower than in II and thus, the operational costs are lower too.

Additionally, a fourth Scenario was created, similar to Scenario III, but with different weight

criteria, where the results were exactly the same.
Finally, the heat produced by the solar panels had such a small influence in the total heating demand that was created a single figure with the behaviour of this variable. Only Scenarios II and III produced heat considering the solar contribution and it was equal for both situations.
Figure 5.27 represents the heat produced from the conversion of solar radiation.

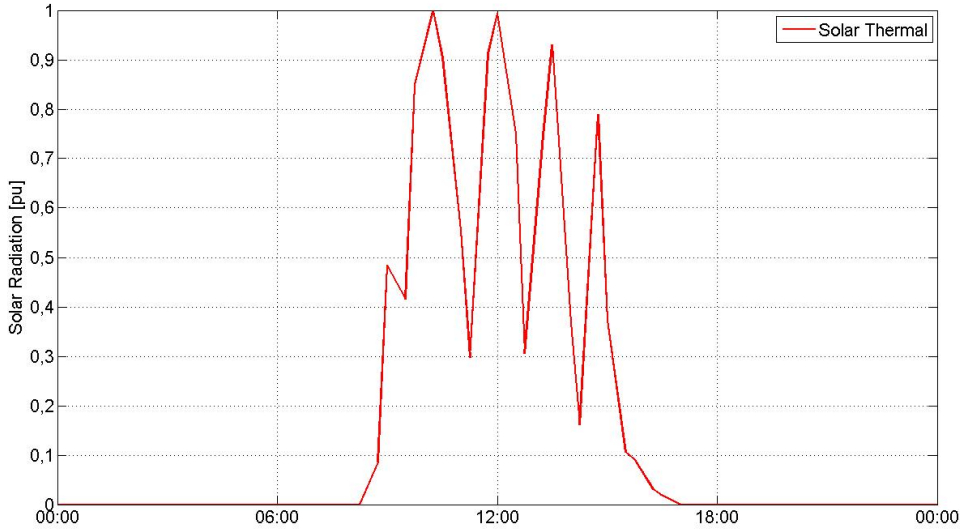

Figure 5.27: Solar contribution for heat production for Scenarios II and III.

The results provide a clear minimization of energy consumption on the total cooling demand with a smoother behaviour of consumption, that demonstrate that the building can be consuming more than it should be. On the other hand, the introduction of a CHP does not proof much benefits in the two first scenarios, as the consumption of primary energy sources grow as observable on Figure 5.23 and, consequently, its emissions grow as well, as can be seen on Figure 5.24. On the contrary, on Scenario III (and IV), with a higher CHP efficiency for the cogeneration of heat, it presents the most satisfying results, compared with the other scenarios.

Chapter 6

Conclusions and Future Work

6.1 Contributions

This dissertation aims the energy flow optimization of a multi energy carrier system combining a training and prediction algorithm for the characterization of demands, and an optimization algorithm with the objective of calculating the optimal operation of the CTM building for a 24 hour period. The optimization process took also into account the minimization of the CO_2 emissions and operational costs.

The first step required the characterization of the demands of the building through the application of ANFIS creating predictive models of the chosen variables. Considering the resulting RMSE of each model, the algorithm revealed to be effective and satisfying.

Secondly, the proposed methodology focused on the energy flow system optimization throughout the characterization of the efficiency of the equipment involved, as well as the mathematical formulation of the system and the use of the SQP algorithm that calculated the optimal operation, applying a fitness function with the goal of minimizing the chosen criteria – energy, costs and CO_2 emissions minimization. Three scenarios considering different weight criteria and CHP efficiency were tested with the most satisfying results corresponding to Scenario III. In this scenario, all the criteria were minimized with the exception of the operational costs, that were equal for each situation.

6.2 Future Work

During the different steps of the development of this dissertation, many possibilities and approaches could have been made. Most of the times, due to time restriction, either in the creation of the models, or in the equipment's efficiency characterization, or in the optimization process, different possible improvement approaches could have been taken and thus, as follows, are presented some improvement ideias.

- Characterization of the Demand

  In this step, the types of meteorological data were defined as the best ones to characterize each demand - the temperature outside of the building and the solar radiation, were always present. As so, choosing different meteorological data, within the many possibilities that the meteorological station offers, could result on more complete models, more close to reality.
  Additionally, in the deffinition of the internal parameters of the ANFIS algorithm, the % of data set to training and validation are 70% and 30%, respectively. The training and checking were selected in chronological order - first part is used for training and last part for validation. A new possibility could relay on a different % of data selected for validation and training, as well as the order for what they are chosen for - not in a chronological order but random for example - that could include a wider variety of data and thus, better models.

- Characterization of Equipment

  The equation that defined the chiller's efficiency resulted from a multiple linear regression that included the set point temperature and the temperature outside the building as dependent variables. The temperature outside the building is easy to predict, but the set point temperature it's not. Consequently, a different approach could involve other variables easier to predict to facilitate the optimization process.
  With exception of the chiller, the other equipment's efficiency values were defined with a general value, that not exactly corresponds to the reality as the efficiency changes constantly. As so, a different approach can be made in this topic with the definition of an equation that defines the equipment's efficiency at any moment.

- Optimization

  The 24 hour prediction was made to a day where the production was already known in order for the comparison between the calculated production and the real one to be possible. Hereafter, a 24 hour prediction of a day in the future would be a necessary step to strengthen the proposed methodology in this dissertation. Another relevant restricition of the presented optimization process, is the limited range of meteorological contitions that took part of the process. More experiments could be done in different conditions to test the algorithms in every possible conditions.

Bibliography

[1] G. Acampora, C. Landi, M. Luiso, and N. Pasquino. Optimization of energy consumption in a railway traction system. *International Symposium on Power Electronics, Electrical Drives, Automation and Motion, 2006. SPEEDAM 2006*, 2006:1121–1126, 2006.

[2] G. Blanco, R. Gerlagh, S. Suh, J. Barrett, H. C. de Coninck, C. F. Diaz Morejon, R. Mathur, N. Nakicenovic, A. Ofosu Ahenkora, J. Pan, H. Pathak, J. Rice, R. Richels, S. J. Smith, D. I. Stern, F. L. Toth, and P. Zhou. Drivers, Trends and Mitigation. *Climate Change 2014: Mitigation of Climate Change. Contribution of Working Group III to the Fifth Assessment Report of the Intergovernmental Panel on Climate Change*, Chapter 5:351–412, 2014.

[3] Ulrich Boeke and Leopold Ott. Impact of a 380 V DC Power Grid Infrastructure on Commercial Building Energy Profiles. 2014.

[4] Helena Bozic. Optimization of Energy Consumption and Energy Efficiency Measures with MARKAL Model. *2007 International Conference on Clean Electrical Power*, pages 299–301, 2007.

[5] M. Brenna, M. C. Falvo, F. Foiadelli, L. Martirano, F. Massaro, D. Poli, and A. Vaccaro. Challenges in energy systems for the smart-cities of the future. *2012 IEEE International Energy Conference and Exhibition, ENERGYCON 2012*, pages 755–762, 2012.

[6] Ulrich Cubasch, Donald Wuebbles, Deliang Chen, Maria Cristina Facchini, David Frame, Natalie Mahowald, and Jan-Gunnar Winther. Introduction. *Climate Change 2013: The Physical Science Basis. Contribution of Working Group I to the Fifth Assessment Report of the Intergovernmental Panel on Climate Change*, pages 119–158, 2013.

[7] European Commission. *Green paper - Towards a European Strategy for the Security of Energy Supply*. Number October. 2001.

[8] Andreas Goldthau. The Handbook of Global Energy Policy. pages 225–282, 2013.

[9] Dennis J Hartmann, Albert M G Klein Tank, Matilde Rusticucci, Lisa V Alexander, Stefan Brönnimann, Yassine Abdul-Rahman Charabi, Frank J Dentener, Edward J Dlugokencky, David R Easterling, Alexey Kaplan, Brian J Soden, Peter W Thorne, Martin Wild, and Panmao Zhai. Observations: Atmosphere and Surface. *Climate Change 2013: The Physical*

Science Basis. Contribution of Working Group I to the Fifth Assessment Report of the Intergovernmental Panel on Climate Change, pages 159–254, 2013.

[10] E V Huntington. A New Set of Independent Postulates for the Algebra of Logic with Special Reference to Whitehead and Russell's Principia Mathematica. *Proceedings of the National Academy of Sciences of the United States of America*, 18(2):179–180, 1932.

[11] Pekka Huovila, Mia Ala-Juusela, Luciana Melchert, Stéphane Pouffary, Dr. Chia-Chin Cheng, Diana Urge-Vorsatz, Sonja Koeppel, Niclas Svenningsen, and Peter Graham. Buildings and Climate Change - Summary for Decision-Makers. *UNEP*, 2013.

[12] IEA. *World Energy Outlook 2012*. 2012.

[13] IEA. Energy and climate change. *World Energy Outlook Special Report*, pages 17–31, 2015.

[14] IEA, M. Basu, Aqeel Ahmed Bazmi, Gholamreza Zahedi, Bruckner T., I.A. Bashmakov, Y. Mulugetta, H. Chum, A. de la Vega Navarro, J. Edmonds, A. Faaij, B. Fungtammasan, A. Garg, E. Hertwich, D. Honnery, D. Infield, M. Kainuma, S. Khennas, S. Kim, H.B. Nimir, K. Riahi, N. Strachan, R. Wiser, X. Zhang, Cec, Kat Cheung, Heejin Cho, Amanda D Smith, Pedro Mago, Climate Works Australia, Nelson Fumo, Louay M. Chamra, IEA, International Energy Agency, International Energy Agency (EIA), C.N. Jardine, G.W. Ault, Xi Zhuo Jiang, Danxing Zheng, Yue Mi, Benjamin Kroposki, Bobi Garrett, Stuart Macmillan, Brent Rice, Connie Komomua, Mark O Malley, Dan Zimmerle, Benjamin Kroposki, H. Lund, B. Möller, B.V. Brian Vad Mathiesen, A. Dyrelund, Rasmus Lund, B.V. Brian Vad Mathiesen, H. Lund, D. Connolly, H. Wenzel, P.a. Østergaard, B. Möller, S. Nielsen, I. Ridjan, P. Karnøe, K. Sperling, F.K. Hvelplund, Gonalo Mendes, Christos Ioakimidis, Paulo Ferrão, Linda Olsson, Elisabeth Wetterlund, Mats Söderström, Abigail D. Ondeck, Thomas F. Edgar, Michael Baldea, Simon Perry, Jiří Klemeš, Igor Bulatov, Energy Policies, I E a Countries, Special Report, Intergovernmental Panel, Climate Change, Behnaz Rezaie, Marc a. Rosen, S. Rinne, S. Syri, Ralph Sims, Pedro Mercado, Wolfram Krewitt, Gouri Bhuyan, Damian Flynn, Hannele Holttinen, Gilberto Jannuzzi, Smail Khennas, Yongqian Liu, Lars J. Nilsson, Ogden Joan, Kazuhiko Ogimoto, Mark O'Malley, Hugh Outhred, Øystein Ulleberg, Frans van Hulle, Subho Upadhyay, M. P. Sharma, Debalina Sengupta, Ralph W Pike, IEA, Kathleen Vaillancourt, GianCarlo Tosato, D.G Victor, D Zhou, E.H.M Ahmed, P.K Dadhich, H-H Oliver, Rongner, K. Sheikho, and M Yamaguchi. Integrating waste and renewable energy to reduce the carbon footprint of locally integrated energy sectors. *Applied Energy*, 15(11):1–9, 2015.

[15] International Energy Agency. Capturing the Multiple Benefits of Energy Efficiency: Executive Summary. *Capturing the Multiple Benefits of Energy Efficiency*, pages 18–25, 2014.

[16] IPCC. Buildings.In: Climate Change 2014: Mitigation of Climate Change: Contribution of Working Group III to the Fifth Assessment Report of the Intergovernmental Panel on Climate Change. *Ipcc*, 33:1–44, 2014.

[17] IPCC. Climate Change 2014 Synthesis Report Summary Chapter for Policymakers. *Ipcc*, page 31, 2014.

[18] J. S. R. Jang. ANFIS - Adaptive-Network-Based Fuzzy Inference System, 1993.

[19] K Kampouropoulos and J J Cárdenas. An Energy Prediction Method using Adaptive Neuro-Fuzzy Inference System and Genetic Algorithms. *IEEE ISIE conf.*, (May):1–6, 2013.

[20] Konstantinos Kampouropoulos, Fabio Andrade, Enric Sala, and Luis Romeral. Optimal control of energy hub systems by use of SQP algorithm and energy prediction. *Proceedings, IECON 2014 - 40th Annual Conference of the IEEE Industrial Electronics Society*, pages 221–227, 2014.

[21] Jens Laustsen. Energy Efficiency Requirements in Building Codes, Energy Efficiency Policies for New Buildings. *Inernational Energy Agency*, (March):71, 2008.

[22] Mohsen Mahoor, Tooraj Abbasian Najafaabadi, Farzad Rajaei Salmasi, and Senior Member. A smart street lighting control system for optimization of energy consumption and lamp life. *The 22nd Iranian Conference on Electrical Engineering (ICEE 2014), May 20-22, 2014, Shahid Beheshti University*, (Icee):1290–1294, 2014.

[23] Peter Meckler, Frank Gerdinand, Roland Weiss, Ulrich Boeke, and Anton Mauder. Hybrid switches in protective devices for low-voltage DC grids at commercial used buildings. *27th International Conference on Electrical Contacts, June 22 – 26, 2014, Dresden, Germany*, pages 120–125, 2014.

[24] T. Pu and Bai J. Predictive Model of Energy Consumption in Beer Production. *Journal of Engineering Science and Technology Review*, 2:145–149, 2013.

[25] Samir Sahyoun, Cale Nelson, Seddik M. Djouadi, and Teja Kuruganti. Control and room temperature optimization of energy efficient buildings. *2012 IEEE International Conference on Control Applications*, pages 962–967, 2012.

[26] Sven Teske, Arthouros Zervos, and Oliver Schafer. Energy [r]evolution - A sustainable world energy outlook. pages 1–96, 2007.

[27] United Nations Development Programme UNDP. *Human Development Report 2015 Work for Human Development*. 2015.

[28] U.S. Department of Energy. Energy Efficiency Trends in Residential and Commercial Buildings. *Energy*, (October):1–32, 2008.

[29] D.G. Vaughan, J.C. Comiso, I. Allison, J. Carrasco, G. Kaser, R. Kwok, P. Mote, T. Murray, F. Paul, J. Ren, E. Rignot, O. Solomina, K. Steffen, and T. Zhang. Observations: Cryosphere. *Climate Change 2013: The Physical Sci- ence Basis. Contribution of Working Group I to the Fifth Assessment Report of the Intergovernmental Panel on Climate Change*, pages 317–382, 2013.

[30] Alberto Vergnano, Carl Thorstensson, Bengt Lennartson, Petter Falkman, Marcello Pellicciari, Francesco Leali, and Stephan Biller. Modeling and optimization of energy consumption in cooperative multi-robot systems. *Tase*, 9(2):423–428, 2012.

[31] Moomaw Bill. W. Energy Supply: Overview of current sources of investments and financing, energy Consumptions and GHG emissions under reference and mitigation scenarios. 2007.

[32] R. Weiss, L. Ott, and U. Boeke. Energy efficient low-voltage DC-grids for commercial buildings. *2015 IEEE 1st International Conference on Direct Current Microgrids, ICDCM 2015*, pages 154–158, 2015.

[33] Bernd Wunder. 380V DC in Commercial Buildings and Offices. *VICOR seminar 2014, Fraunhofer Institute of Integrated Systems and Device Technology*, page 71, 2014.

[34] Bernd Wunder, Leopold Ott, Marek Szpek, Ulrich Boeke, and Dr. Roland Weiss. Energy Efficient DC-Grids for Commercial Buildings. *IEEE 36th International Telecommunications Energy Conference (INTELEC)*, pages 1–8, 2014.

[35] Yang Gao, E. Tumwesigye, B. Cahill, and K. Menzel. Using data mining in optimisation of building energy consumption and thermal comfort management. pages 434–439, 2010.